Altered Expression of Neuronal Cell Adhesion Molecules Induced by Nerve Injury and Repair

Joanne K. Daniloff,* Giovanni Levi,* Martin Grumet,*
François Rieger,‡ and Gerald M. Edelman*

*The Rockefeller University, New York 10021; and ‡Groupe de Biologie et Pathologie Neuromusculaires, Institut National de la Santé et de la Recherche Médicale, Paris, France

Abstract. Peripheral nerve injury results in short-term and long-term changes in both neurons and glia. In the present study, immunohistological and immunoblot analyses were used to examine the expression of the neural cell adhesion molecule (N-CAM) and the neuron–glia cell adhesion molecule (Ng-CAM) within different parts of a functionally linked neuromuscular system extending from skeletal muscle to the spinal cord after peripheral nerve injury. Histological samples were taken from 3 to 150 d after crushing or transecting the sciatic nerve in adult chickens and mice. In unperturbed tissues, both N-CAM and Ng-CAM were found on nonmyelinated axons, and to a lesser extent on Schwann cells and myelinated axons. Only N-CAM was found on muscles. After denervation, the following changes were observed: (*a*) The amount of N-CAM in muscle fibers increased transiently on the surface and in the cytoplasm, and in interstitial spaces between fibers. (*b*) Restoration of normal N-CAM levels in muscle was dependent on reinnervation; in a chronically denervated state, N-CAM levels remained high. (*c*) After crushing or cutting the nerve, the amount of both CAMs increased in the area surrounding the lesion, and the predominant form of N-CAM changed from a discrete M_r 140,000 component to the polydisperse high molecular weight embryonic form. Anti–N-CAM antibodies stained neurites, Schwann cells, and the perineurium of the regenerating sciatic nerve. Anti–Ng-CAM antibodies labeled neurites, Schwann cells and the endoneurial tubes in the distal stump. (*d*) Changes in CAM distribution were observed in dorsal root ganglia and in the spinal cord only after the nerve was cut. The fibers within affected dorsal root ganglia were more intensely labeled for both CAMs, and the motor neurons in the ventral horn of the spinal cord of the affected segments were stained more intensely in a ring pattern by anti–N-CAM and anti–Ng-CAM than their counterparts on the side contralateral to the lesion.

Taken together with the previous studies (Rieger, F., M. Grumet, and G. M. Edelman, *J. Cell Biol.* 101:285–293), these data suggest that local signals between neurons and glia may regulate CAM expression in the spinal cord and nerve during regeneration, and that activity may regulate N-CAM expression in muscle. Correlations of the present observations are made here with established events of nerve degeneration and suggest a number of roles for the CAMs in regenerative events. Such correlations may have practical applications in the study of nerve repair particularly in view of the function of CAMs in mediating cell–cell adhesion leading to tissue structures.

After peripheral nerve damage, normal biochemical and morphological relationships between cell somata, their axonal and dendritic processes, and their terminations in targets such as muscle are disturbed both proximal and distal to the site of injury (1, 11, 29, 66, 67). Only part of this damage is reversed in the regenerative process that resembles residual or reactivated developmental mechanisms (2, 41, 44, 66).

Recent studies (17, 18, 62, 70) suggest that cell–cell interactions mediated by cell adhesion molecules (CAMs)[1] are key mechanisms in regeneration as well as in development. The neural CAM, N-CAM, and the neuron–glia CAM, Ng-CAM, undergo developmentally linked changes or cell surface modulations that can affect their function (25). N-CAM plays a key role in binding of neurons to neurons (49) and to striated muscle cells (40, 72). N-CAM on neurons binds homophilically to N-CAM on apposing neurons (49). During brain development, the sialic acid-rich embryonic (E) form of N-CAM undergoes conversion to adult (A) forms containing lower amounts of sialic acid (15, 33), and the A forms show increased rates of binding (49). It has been suggested that E to A conversion is one means of stabilizing contacts between neurons (24). Consistent with this idea, the relative concentration of N-CAM decreases sharply during

1. *Abbreviations used in this paper*: A form, adult form; CAM, cell adhesion molecule; ChAT, choline acetyltransferase; DRG, dorsal root ganglion; E form, embryonic form; N-CAM, neural CAM; Ng-CAM, neuron–glia CAM.

the embryonic development of muscle and, with time, the A form predominates in most loci (70). N-CAM has been localized in the adult neuromuscular junction (17, 18, 70) and may be involved in stabilization of nerve–muscle contacts and maturation of motor endplates (70).

In contrast to N-CAM, which is already present in the blastoderm, Ng-CAM is first seen on postmitotic neurons (38, 76); it participates in heterophilic binding between neurons as well as between neurons and glia. The expression of Ng-CAM during development is correlated with the migration of neurons along glia, with neurite outgrowth during tract formation, and with neurite fasciculation (21, 38, 50, 76).

Modulation of the two neuronal CAMs at the cell surface appears to result from a series of signals at particular neural sites and these signals depend upon tissue integrity. The normal levels of N-CAM are altered, for example, by alterations of connectivity. After the sciatic nerve is severed, the relative amounts of N-CAM on extrajunctional regions of the muscle surface increase dramatically, while staining at the motor endplates is diminished (17, 18, 70). The distribution and amount of the acetylcholine receptor and N-CAM change in parallel, suggesting either that the two molecules interact or that their regulation is linked (18, 70). It has been shown that the expression of Ng-CAM in PC12 pheochromocytoma cells is selectively enhanced by nerve growth factor (9, 33), and this factor is known to play a role in regenerative responses in sensory neurons (58, 75, 78).

In the present study, we describe in detail the extent and timing of changes in CAM expression brought about by cutting or crushing the adult sciatic nerve, and compare these changes to CAM expression in normal tissues. Changes were noted at all levels of connectivity from the hindlimb to the spinal cord. The observed changes in CAM expression were correlated with known metabolic and cellular responses to injury for up to 150 d after injury. The data indicate that expression of different CAMs changes in a locally characteristic fashion in different anatomic neighborhoods after interruption of the connectivity of a linked neuromuscular system.

Materials and Methods

Experimental Design

Young adult (3 wk of age) white Leghorn chickens and C57 Bl/6J mice (8 wk of age) were used. Animals were anesthetized with chloral hydrate (8%; 0.33 ml/100 g body weight) and were subjected to a unilateral crush or cut of the sciatic nerve equidistant between the greater trochanter and lateral condyle of the femur. This position established roughly equal distances between the lesioned nerve, its central (proximal) process, and its normal termination in the calf of the leg, and helped us to identify the lesion site later. Although the length of the degenerating nerve has a profound effect on the efficacy of regeneration (27, 45, 79), damage to the nerve at this site has previously been shown to result in efficient regeneration (66, 69).

The sciatic nerves of chickens were crushed for ~3 s with flat, blunt-tipped forceps (2-mm tip) and animals were sacrificed after 3, 10, 20, 30, and 50 d. The sciatic nerves of mice were crushed with fine watchmaker's forceps and the animals were sacrificed after 3, 7, 19, 30, and 50 d. The site of the crush was located morphologically and with the help of an overlying suture. Chicken nerves were transected by removing a 2-mm segment and the animals were sacrificed after 3, 10, 20, 30, 60, and 150 d.

After sacrifice, tissues were removed for anatomical or biochemical analyses. The gastrocnemius muscles and sciatic nerves of the chickens, and the gastrocnemius, soleus, and extensor digitorum longus muscles and sciatic nerves of the mice were assayed. Spinal cords and dorsal root ganglia (DRGs) from spinal segments 23–26 were examined after the dorsal and ventral roots were cut away from the spinal cord. Results with control tissues taken from the contralateral side of experimental animals were identical to corresponding tissues of unoperated animals. The spinal cord and ganglia from brachial segments also served as controls.

The battery of antibodies used both to label tissue sections and in immunoblot analyses included polyclonal and monoclonal antibodies prepared against N-CAM (51) and Ng-CAM (37, 39). Polyclonal antibodies raised against S100 protein were used to label Schwann cells (52, 53, 73). Antibodies to beef brain S100 were prepared using a complex of the protein with methylated BSA (46). Rabbits were immunized with 1 mg of S100 protein (Calbiochem-Behring Corp., La Jolla, CA) mixed with 1 mg methylated BSA (Sigma Chemical Co., St. Louis, MO) in PBS; the first injection was in complete Freund's adjuvant; the second injection, 2 wk later, was in incomplete Freund's adjuvant; subsequent injections were in PBS. Rabbits were bled 2 wk after the third injection and IgG was prepared as described (10).

Preservation of Tissues for Histology

Fresh samples of muscle were removed, immersed in embedding compound (Tissue-Tek; Miles Scientific, Naperville, IL), and frozen in cold isopentane. Frozen sections of the muscle (8 μm thick) were cut in a cryostat, collected on gelatin-coated slides, dried, and stored overnight at 4°C. Sections were fixed for 1 h (2.5% paraformaldehyde/0.02% glutaraldehyde/0.1 M phosphate buffer [pH 7.0]), immersed for 15 min in a PBS solution containing 0.1 M glycine, washed in PBS for 20 min, and incubated with primary antibodies (10–20 μg/ml) in the presence of 5% goat serum.

Fresh pieces of sciatic nerves were placed on filter paper and fixed as described above. The spinal cord and DRGs were dissected from chickens that had been transcardially perfused with the same fixative for 20 min; tissues were postfixed for 20 min and immersed overnight in phosphate-buffered sucrose (30%). After equilibrating in Lipshaw's embedding medium, the tissues were frozen. Sections (10 μm thick) were cut and allowed to dry overnight at room temperature before incubation with primary antibodies.

Immunofluorescent Labeling of Antigens

Tissue sections were incubated in PBS containing 5% nonimmune goat serum for 20 min at room temperature, then overnight in the appropriate antibodies. Bound monoclonal antibodies were visualized after sequential incubation with rabbit anti-mouse IgG (1:50; Miles Laboratories Inc., Elkhart, IN) and rhodamine-conjugated goat anti-rabbit IgG (1:100; Cappel Laboratories, Cochranville, PA). Polyclonal antibodies were visualized by incubation with rhodamine-conjugated IgG (1:100). When double-labeling was performed, tissue sections were incubated overnight at room temperature in a mixture containing both polyclonal anti-Ng-CAM and monoclonal anti-N-CAM (No. 1) antibodies (51). After washing four times with PBS, bound monoclonal antibodies were visualized by sequential incubation in biotinylated horse anti-mouse IgG and avidin-fluorescein-conjugated goat anti-horse IgG (1:100; Cappel Laboratories). Polyclonal antibodies were visualized with rhodamine-conjugated goat anti-rabbit IgG as described above. After washing, labeled preparations were mounted in 10% PBS/0.1% paraphenylene diamine (Sigma Chemical Co.) in glycerol. Photomicrographs were taken with a Zeiss photomicroscope equipped with the appropriate filters for fluorescein and rhodamine optics. Double-labeled sections are indicated in all figures by a prime after the letter.

Preparation of Tissue Lysates

Mice were sacrificed by cervical dislocation, and chickens by administering an overdose of chloral hydrate anesthetic. Muscles and nerves were removed and immediately frozen. In mice, care was taken to separate the proximal and distal nerve segments from the site of the crush; in chickens, ~3 mm of the nerve was taken from either the region surrounding the crush site or the area of the scar that had formed between the two cut stumps. DRGs were severed from the spinal cord and then frozen individually. The spinal cord was removed in ice-cold calcium-magnesium free medium, divided longitudinally in half, cut into 0.3-mm slices with a tissue chopper (Brinkman Instruments, Westbury, NY), and frozen. Half of the slices were analyzed in toto. Ventral horns were microdissected from the remaining slices, pooled, and frozen.

For immunoblot analyses, muscles were cut in small pieces and homogenized in a glass Dounce homogenizer in 5 vol of boiling PBS containing 1% SDS and 0.2 M EDTA. The samples were centrifuged at 100,000 *g* for

20 min and the protein concentrations of the supernatant fractions were determined (59). Neural tissues were homogenized in cold PBS containing Trasylol (220 kIU/ml; Mobay Chemical Corp., Pittsburgh, PA) and centrifuged at 100,000 *g* for 10 min at 4°C. The supernatant was discarded and the pellet was extracted in PBS-Trasylol containing 0.5% Nonidet P-40. After centrifugation, the supernatant was collected and the protein concentrations were determined (59).

Immunoblots

Tissue extracts were diluted to equal protein concentrations; the samples were boiled 3 min and resolved by SDS PAGE on 6.5% polyacrylamide gels. After transfer to nitrocellulose paper (80), the blots were reacted sequentially with 50 μg of polyclonal or monoclonal antibodies and ^{125}I-labeled protein A (1×10^6 cpm) as described previously (38, 39, 70). The results were visualized by autoradiography. To quantitate the amount of N-CAM on immunoblots, regions corresponding to M_r 140,000–200,000 were excised and amounts of ^{125}I-protein A were measured by gamma spectroscopy as previously described (50). To obtain specific binding, background levels from control areas containing no N-CAM were subtracted.

Immunoprecipitation and Neuraminidase Treatment

Muscle extracts containing equivalent amounts of protein were diluted 1:7 with PBS containing a final concentration of 1% Nonidet P-40 (PBS/Nonidet P-40) and incubated overnight with Sepharose beads (Pharmacia Fine Chemicals, Piscataway, NJ) coupled to polyclonal anti-N-CAM IgG. The coupled beads were washed four times in PBS/Nonidet P-40 and for neuraminidase treatment, the beads were then washed once in PBS and resuspended in buffer containing 0.1 M sodium acetate, 0.2 mM EDTA, and 2 mM $CaCl_2$ (pH 5.0) as previously described (20). Identical samples were then incubated at 37°C for 4 h in the presence or in the absence of neuraminidase from *Vibrio cholerae* (Calbiochem-Behring Corp.; 1 U/ml) and then an equal volume of sample buffer was added and the samples were boiled 3 min. Proteins were resolved by SDS PAGE as described above.

Recovery of Function

As determined by periodic observations, the hindlimbs of chickens and mice were severely disabled for several days after a crush of the sciatic nerve. Experimental chickens had partially regained function in the operated limb after 50 d and mice had a normal appearing gait after 21 d. After nerve transection, the function of the limb was only partially regained in the experimental animals and it was observed that compensatory strategies were adopted for walking. By 120 d, some volitional control of the hindlimb was restored in mice, although it was restricted to gross movement of the leg with little control of distal movement. Most chickens used the knee joint of the flexed hindlimb to bear the weight of the affected side of the body.

To estimate the amount of reinnervation in mouse gastrocnemius muscles, biochemical levels of choline acetyltransferase (ChAT) activity were assayed using the rapid radiochemical assay of Fonnum (30). In a control experiment, naphthyl vinyl pyridine hydrochloride (Calbiochem-Behring Corp.) was used (final concentration 10^{-4} M) to inhibit ChAT synthesis; nonspecific enzyme activity was then subtracted from the raw data. Homogenates were prepared from each of three control and experimental gastrocnemius muscles, each taken 0, 3, 19, or 30 d after the sciatic nerves were crushed or cut. In a third group, the proximal nerve segment was sutured to the overlying dermis (reverse suture) to completely prevent muscle reinnervation (41, 44, 45). A total of 36 animals were studied and each sample was run in triplicate.

Results

Anatomical Distribution of CAMs After Nerve Injury

Two general paradigms, nerve compression and nerve transection, have been extensively used to investigate regeneration in vertebrates (4, 41, 66, 69). In this study, we have used histochemical and biochemical methods to examine changes in the amounts, forms, and cellular distribution of CAMs in muscle, nerve, and spinal cord after transection or compression of the sciatic nerve. Fig. 1 shows an immunocytochemical comparison of low magnification of normal, crushed, and transected sciatic nerves, which provides an overview of the changes in morphology and CAM distribution that are induced 10 d after lesions, a time intermediate between degenerative and regenerative events.

In longitudinal sections of normal sciatic nerves, low levels of Ng-CAM (Fig. 1 *A*) and N-CAM (Fig. 1 *A'*) were observed. After 10 d, staining for both Ng-CAM and N-CAM was increased relative to control nerves (compare Figs. 1 *A* and 1 *A'* to Figs. 1 *B* and 1 *B'*). The intensity of staining at the site of the crush was similar to the areas on the local adjoining regions, both proximal and distal to the lesion. In contrast to the crush procedure, 10 d after nerve transection (Fig. 1, *C* and *C'*), neurites in the proximal stump that extended from the original nerves were intensely stained for Ng-CAM (Fig. 1 *C*). Only faint Ng-CAM staining was observed, however, in the distal portions of the nerve. A club-like swelling of the stump, originally described by Ramon y Cajal (66), was formed by neurites moving distally. Very few fibers had crossed the gap to enter the distal stump by 10 d. There was intense N-CAM staining in the proximal stump; the distal stump and the gap between the stumps expressed N-CAM to a lesser degree (Fig. 1 *C'*). Before the perineurium was restored, the non-neural cells that comprised the scar region were N-CAM positive and were either low or negative for Ng-CAM. At this level of resolution, we were not able to rule out the possibility that other elements besides neurites and Schwann cells, including fibroblasts, lymphocytes, macrophages, and other reactive cells (50, 60), also might have been stained for N-CAM as a result of inflammatory processes.

To assess the changes in the target tissues which resulted from these two types of lesion in the nerve, we examined the expression of N-CAM in the gastrocnemius, soleus, and extensor digitorum longus muscles of mouse and chicken at various times after nerve injury. As shown previously (17, 70), normal adult mouse muscles contain low levels of N-CAM in the connective tissues and on the surfaces of myofibers (Fig. 2 *A*). N-CAM was not detected in the cytoplasm of normal muscle fibers. In mice, muscles were examined 3, 7, 19, and 50 d after the sciatic nerve was crushed. At 3 d, a transient increase (17, 70) in N-CAM was observed in the cytoplasm of the muscle, on the myofiber surface, and extracellularly between the fibers (Fig. 2 *B*). In fast twitch muscles, including the gastrocnemius (Fig. 2 *C*) and the extensor digitorum longus (not shown), the level of N-CAM decreased to control levels by 11 d after crush. In a slow twitch muscle (soleus), the normal distribution of N-CAM took ~3 wk to return.

In the chicken, normal adult muscle expressed small amounts of N-CAM extracellularly between muscle fibers (Fig. 2 *G*). Teased, whole-mount preparations of chicken muscle fibers indicated that N-CAM was found at motor endplates (open arrow, inset, Fig. 2 *G*) and on mononucleated cells that probably consisted of both satellite cells (filled arrow in insert) and fibroblastic cells between muscle fibers. These low levels were not artifactual, however, as shown by the fact that staining was completely abolished when antibodies were preincubated with purified antigen before being applied to tissue sections (Fig. 2 *D*).

After a nerve crush in chickens, a transient increase in the amount of N-CAM was observed within the gastrocnemius muscle. The N-CAM was found predominantly within

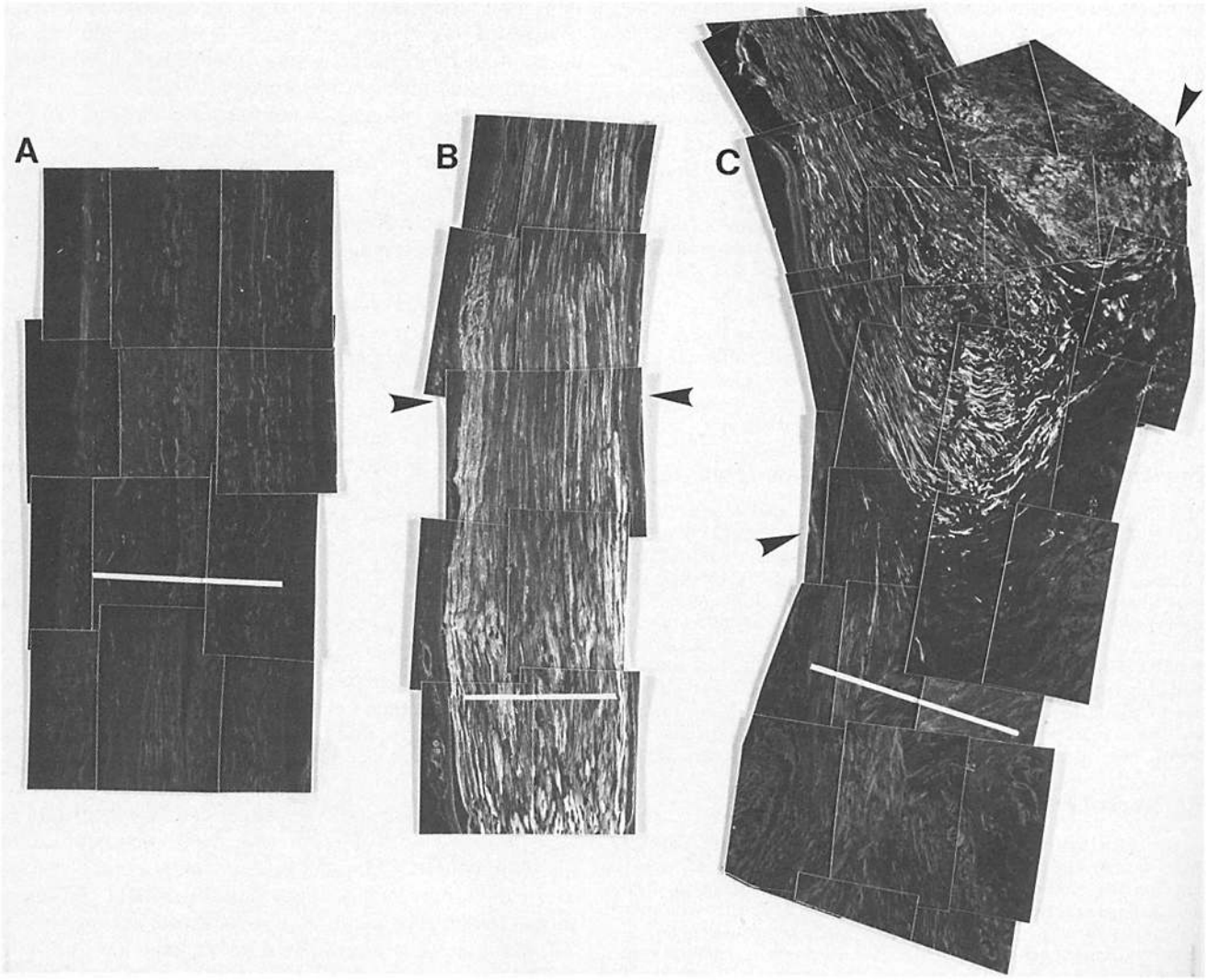

Figure 1. Photomontages of longitudinal sections of normal sciatic nerves (*A* and *A'*), crushed (*B* and *B'*), and cut (*C* and *C'*) nerves 10 d after surgery. The same sections were double-labeled with anti-Ng-CAM (*A–C*) and anti-N-CAM (*A'–C'*) IgG. In each case, the region between the black arrows is the site of the lesion and the white line indicates the approximate location for the photomicrographs of the distal nerve shown in Figs. 3 and 4. In experimental nerves, the intensity of both Ng-CAM (*B* and *C*) and N-CAM staining (*B'* and *C'*) increased, compared with control levels (*A* and *A'*). Many Ng-CAM- (*B*) and N-CAM- (*B'*) positive fibers traversed the compressed region (*black arrows*) to enter the distal nerve by 10 d. In comparison, very few sprouted fibers, labeled with anti-Ng-CAM antibodies in *C*, were observed in the distal stump 10 d after nerve transection. The transected nerve was also more homogeneously labeled for N-CAM (*C'*) than Ng-CAM (*C*). Black bar, 500 μm.

mononucleated cells and in extracellular spaces between muscle fibers (Fig. 2 *E*). Cytoplasmic and surface staining of muscle fibers was also observed although it was less intense than that of the tissues between fibers (Fig. 2 *E*). After 50 d, the pattern of N-CAM staining in the muscle had returned to normal levels (Fig. 2 *F*).

Chicken muscles were also examined 3, 10, 20, 30, 60, and 150 d after nerve transection. A large increase in N-CAM was observed after 10 d in extracellular connective tissues; mononucleated cells of chick muscle and the cytoplasm of the muscle fibers were also stained (Fig. 2 *H*). After 150 d (Fig. 2 *I*), the distribution of N-CAM in chick muscle returned to that of the controls (compare Fig. 2, *G* and *I*).

To determine how the expression of CAMs correlated with the detailed degenerative and regenerative events in the nerve, we examined the time course of CAM expression in the nerve after injury (Figs. 3–7). Longitudinal sections of normal and lesioned nerves taken ~2–3 mm distal to the lesion (see area in Fig. 1 at white line) are shown in Fig. 3. In normal sciatic nerve (Fig. 3, *A* and *B*), Schwann cells, identified by their reactivity with antibodies to S100 protein (Fig. 3 *B*; 52, 53, 73), were also positive for Ng-CAM (Fig. 3 *A*) and N-CAM (Fig. 3 *A'*). This result is consistent with previous observations that nonmyelinating Schwann cells identified morphologically express N-CAM (63) and L1 antigen (28), which appears to be mouse Ng-CAM (9, 34, 38). Staining experiments on whole-mount preparations of teased sciatic nerves also indicated that Schwann cells expressed both N-CAM and Ng-CAM (70a). The specificity of polyclonal antibody staining was tested by preincubating the antibodies with purified Ng-CAM (inset in Fig. 3 *A*) and N-CAM (inset in Fig. 3 *A'*) antibodies before being applied to tissue

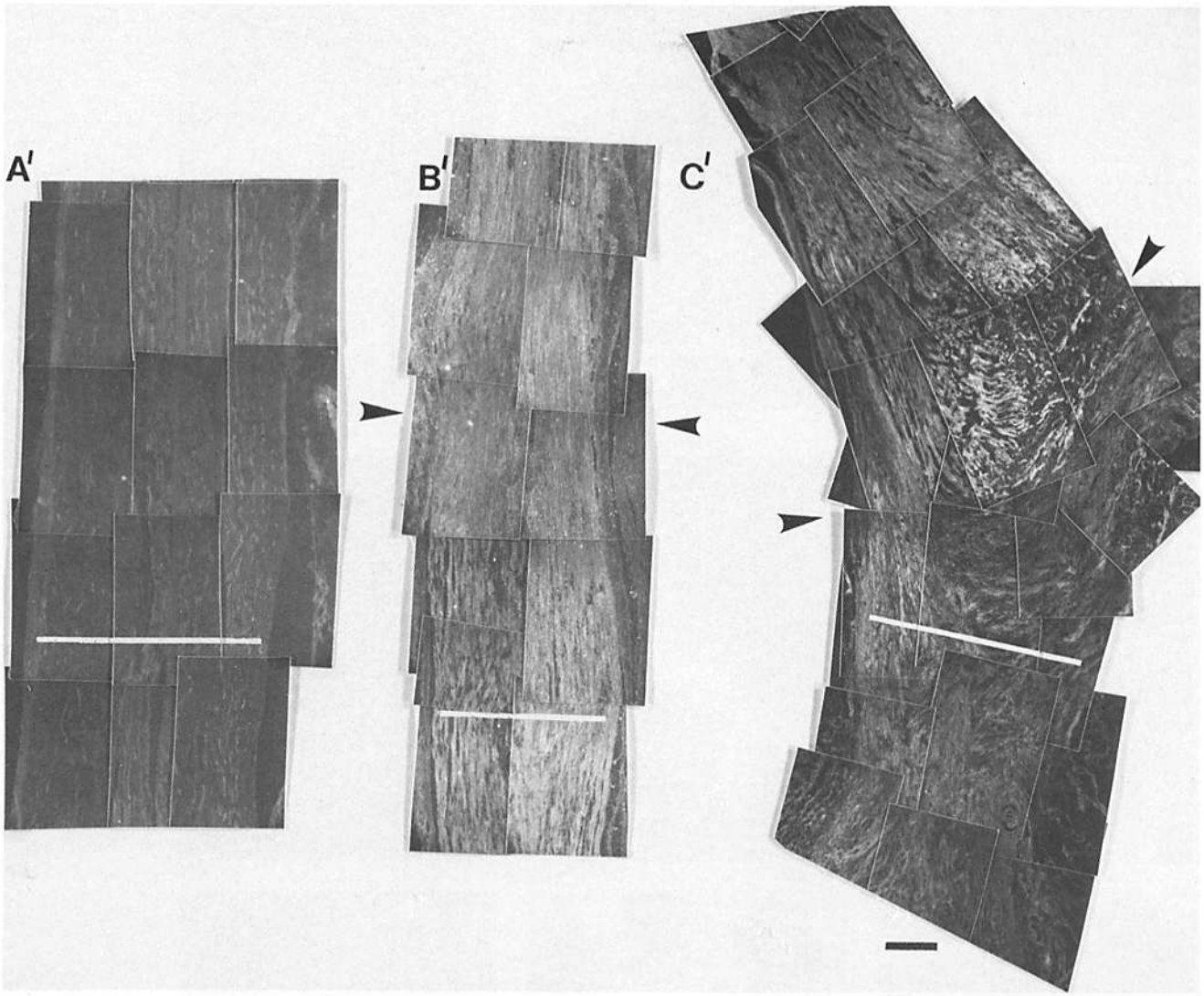

sections. Background staining was tested by incubating tissue sections only in second antibody (inset in Fig. 3 *B*).

Within a few days after a nerve is crushed, the distal stump and 2–3 millimeters of the proximal stump degenerate (66). At this time, Schwann cells proliferate and migrate toward the lesion mainly from the degenerating distal stump (1, 19, 66). We found that 3 d after the nerve was crushed, Schwann cells were intensely labeled with anti–Ng-CAM antibodies (filled arrow in Fig. 3 *C*) and were also N-CAM positive (filled arrow in Fig. 3 *C'*); labeled cells were observed predominantly in the distal segment of both cut and crushed nerves (data not shown). The surface and the cytoplasm, but not the nucleus (data not shown), of these Schwann cells (shown by S100 staining in Fig. 3 *D*) were intensely positive for both CAMs (Fig. 3, *C* and *C'*). Because some CAM-positive cells did not appear to express S100 protein (Fig. 3 *D*), we could not rule out the possibility that non-neural cells other than Schwann cells also expressed or contained the CAMs. The few growing nerve fibers that had penetrated the distal portion of the nerve after 3 d were intensely labeled with antibodies to both CAMs (open arrows in Fig. 3, *C* and *C'*); as expected, no staining for S100 protein was detected on such fibers (Fig. 3 *D*). As shown by early studies, maximal proliferation of Schwann cells should have occurred by this time (1).

The distal stumps of transected nerves were also examined 3 d after the injury. At this time, the amorphous material between the transection and the distal nerve stump was very difficult to fix and stain. However, longitudinally oriented thin walled structures, which appeared to be the endoneurial tubes of the degenerated axons, were faintly labeled with anti–Ng-CAM antibodies 3 d after the nerve was cut (between small arrows in Fig. 3 *E*) and the N-CAM staining was very weak (Fig. 3 *E'*). Schwann cells, identified by S100 staining, were only occasionally observed in the scar region at this time (arrow in Fig. 3 *F*), consistent with the observation that migration of Schwann cells into this region just commences on the third day after injury (66). Empty endoneurial tubes at 3 d (Fig. 4 *A*) subsequently became sites of extensive reinnervation. By 20 d, Ng-CAM-positive fascicles of neurites coursed through the distal stump (Fig. 4 *B*) along cords of S100-protein positive Schwann cells (the bands of Büngner [66]; Fig. 4 *B'*) and Schwann cells expressed only low amounts of Ng-CAM (compare filled ar-

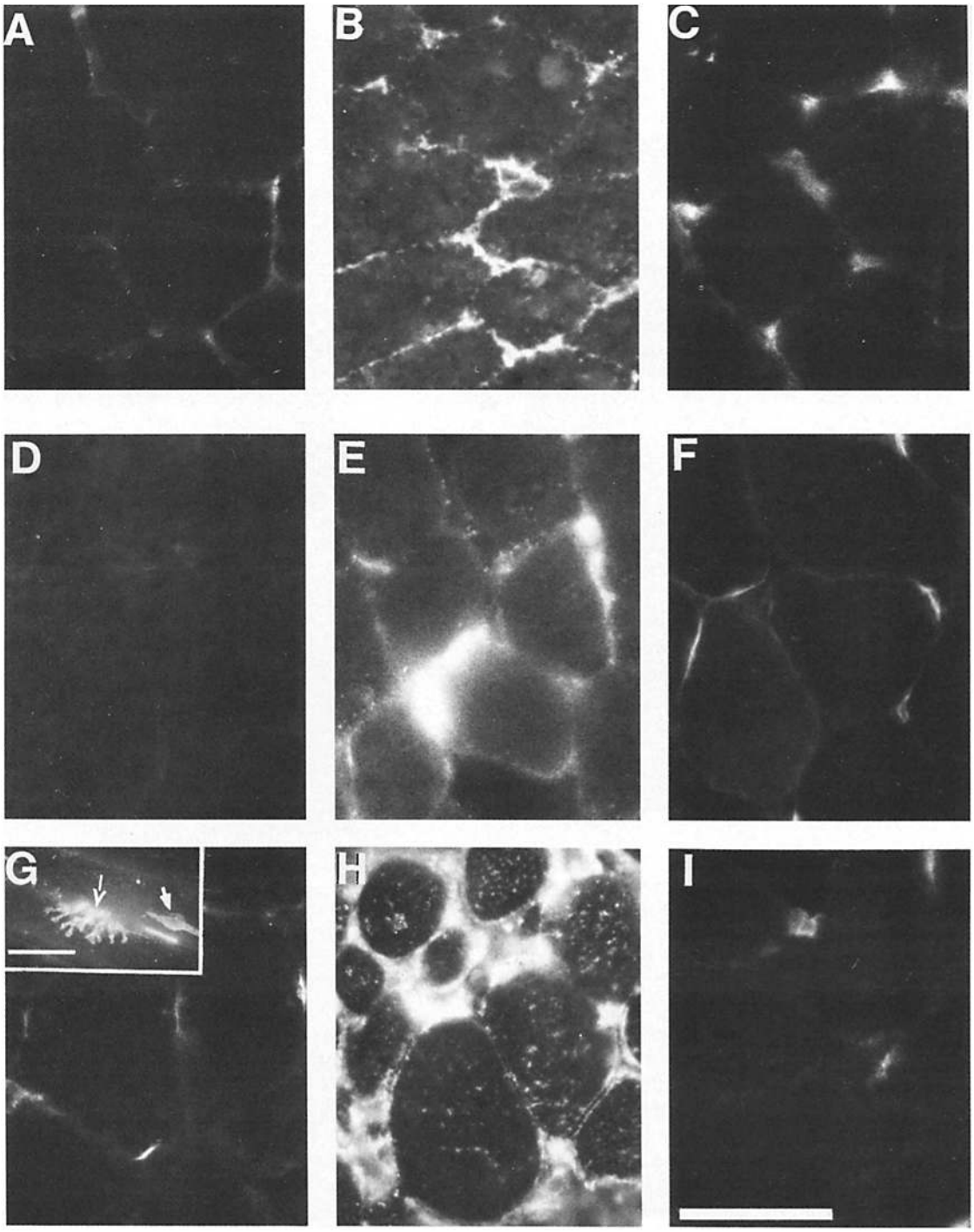

Figure 2. Localization of N-CAM in normal and denervated muscle. Cross-sections of mouse gastrocnemius (*A–C*) and chick gastrocnemius (*D–I*) muscles stained with polyclonal anti-N-CAM IgG. In normal muscles of mice (*A*), the surface of muscle fibers and tissues between fibers were faintly labeled. (*B*) 3 d after crushing the sciatic nerve, the cytoplasm and the surface of muscle fibers were stained and tissues between fibers were intensely labeled with anti-N-CAM antibodies. (*C*) 19 d after the crush, a normal staining pattern was restored. (*D*) As a control for the specificity of antibody staining, normal chicken muscle was stained with anti-N-CAM antibodies that had been incubated with purified chicken N-CAM. (*E*) 10 d after the sciatic nerve was crushed, staining of connective tissues between muscle fibers increased, and the surface of fibers and the cytoplasm were weakly stained. (*F*) 50 d after the crush, the normal staining pattern was restored. (*G*) Surfaces of muscle fibers were faintly labeled in normal chicken muscles. *Inset*, a whole-mount preparation of normal adult teased muscle fibers. The muscle surface was faintly labeled with anti-N-CAM IgG; a motor endplate (*open arrow*) and several mononucleated cells that are probably satellite cells (*filled arrow*) were intensely labeled. (*H*) 10 d after the sciatic nerve was cut, a dramatic increase occurred in the intensity of N-CAM; a normal pattern was restored after 150 d (*I*). Bar, 50 μm.

rows in double-labeled sections of Fig. 4, B and *B'*) and low amounts of N-CAM (not shown).

Transverse sections of normal nerves showed that bundles of non-myelinated axons were intensely labeled with anti-Ng-CAM antibodies, but were only faintly stained with anti-N-CAM antibodies (open arrows in Fig. 5, *A* and *A'*). Schwann cells contained both Ng-CAM and N-CAM (filled arrows in Fig. 5). In contrast, regenerating fibers were brightly stained for Ng-CAM and N-CAM in cross sections of nerves 10 d after the nerve was crushed (open arrows in Figs. 5, *C* and *C'*), and Schwann cells were more intensely labeled for N-CAM than in control preparations (compare Fig. 5, *C'* and *A'*). Staining for S100 protein (Fig. 5 *D*) at this stage revealed abnormal intercellular spaces and a general disruption in Schwann cells that occurred in the distal stump as the myelin (66) was breaking down (compare Fig. 5, *B* and *D*). Gaps formed that were apparent in cross sections (arrowheads in Fig. 5, *C* and *C'*), but these spaces were more prevalent in the distal stump 10 d after the nerve was cut (arrowheads in Fig. 5, *E* and *E'*). The intensity of both Ng-CAM and N-CAM fluorescent staining in distal stumps was elevated at this time (Fig. 5, *E* and *E'*), and an adjacent section stained with antibodies to S100 protein (Fig. 5 *F*) also showed the gaps between Schwann cells.

50 d after crushing the nerve, Ng-CAM approached control levels (Fig. 6 *A*) and the level of N-CAM expression (Fig. 6 *A'*) remained only slightly higher than control levels (compare to Figs. 5, *A* and *A'*). A comparison between histochemical staining (Fig. 6, *A* and *A'*, and Fig. 5, *A* and *A'*), and morphology by phase-contrast microscopy (not shown), indicated that a larger number of CAM-positive, nonmyelinated fibers were present than in controls. Myelination of these fibers begins after 50 d (2, 44, 66), and therefore an increased number of nonmyelinated fibers was expected. The distribution of S100 protein indicated that although Schwann cells were present, they were distributed less densely than in normal controls (compare Fig. 6 *B* to Fig. 5 *B*).

After 150 d, the intensity of Ng-CAM staining in nerves that had been transected returned to nearly normal levels (Fig. 6 *C*); many of the morphological characteristics of the nerve were also normal despite the fact that totally normal conduction velocity and fiber diameter are never achieved at this time (44). Staining for N-CAM was more intense than in controls and the staining pattern was diffuse in cross sections (Fig. 6 *C'*). Bundles of nonmyelinated fibers were denser and larger than in control nerves (compare open arrows in Fig. 6 to Fig. 5) and cross sections stained for S100 protein indicated that large gaps continued to exist between Schwann cells (Fig. 6 *D*). These observations are consistent with the fact that myelination is not extensive even by this time (2, 45, 66).

Patterns of CAM staining in the DRG and spinal cord on the side contralateral to a nerve cut (Fig. 7, *A* and *C*) were compared with the experimental side (Fig. 7, *B* and *D*) 20 d after the sciatic nerve was cut. The distribution of N-CAM and Ng-CAM on normal adult and developing DRG and spinal cord has been reported previously (21). Staining on the nonlesioned side was comparable to normal at all times after a lesion. Fibers and tissues between the cell bodies in the ganglia (64) on the experimental side were more brightly labeled for Ng-CAM (curved white arrow in Fig. 7 *B*) than on the control side (curved white arrow in Fig. 7 *A*). The increased staining for Ng-CAM was most intense after 20 d and began to diminish 30 d after nerve transection. The increase in Ng-CAM staining could have originated from proliferating glial cells, connective tissues, or sprouting fibers (11, 42, 56, 66). No such differences in the DRG were observed in brachial segments used as controls or after a nerve crush (not shown).

Ng-CAM staining of fibers within the ventral horn (indicated by black arrows in Fig. 7, *A* and *B*, and outlined by a dashed white line) of the spinal cord was significantly diminished in intensity compared with the control side. This phenomenon was observed only in animals whose nerve was cut, and only after survival periods of 30 d or less. Such differences were not sustained in animals 150 d after denervation.

The N-CAM staining pattern for motor neurons of the ventral horn (outlined by white dashed line) is shown 20 d after nerve transection on the control (Fig. 7 *C*) and lesioned (Fig. 7 *D*) side. Intense N-CAM staining was observed at the border between the cell surface of motor neurons of the ventral horn (outlined by a white dashed line) and the surrounding neuropil, forming rings around the cells (Fig. 7 *D*). A similar but fainter pattern of N-CAM ring staining was observed within the spinal cord of one animal 3 d after crushing the nerve. At light microscopic levels, we were unable to distinguish whether this staining pattern arose from the cell surface of the motor neurons or from fibers or terminals in the neuropil surrounding the cell. This pattern may have been emphasized on the experimental side because of the general decrease in the intensity of fiber staining in the ventral horn (see Fig. 7 *B*). Similar patterns consisting of accumulations of granules have been visualized around the perimeter of motor neurons with Nissl stains (13, 54).

Biochemical Quantitation of CAMs After Nerve Injury

To quantitate the observed changes in CAM expression, immunoblot analyses were performed and a radiochemical assay of ChAT activity in the target muscles was used to assess the extent of muscle reinnervation.

Muscle. The results presented here together with previous studies (17, 70) suggested that levels of N-CAM in muscles were regulated by innervation. To investigate this issue further, we examined the time course of CAM expression relating it to the extent of innervation, and also determined the levels of N-CAM in a chronically denervated preparation of muscle. As shown previously (17, 70), normal adult mouse muscle contains very low levels of N-CAM that was present as a component of M_r 140,000 observed in immunoblots (Fig. 8 *A*, lanes *1*, *5*, and *9*). After transection of the sciatic nerve in mice, elevated levels of N-CAM occurred in all muscles and remained high for at least 14 d (17, 70). The amount of N-CAM decreased from ~10 times normal levels at 14 d to three times control levels after 120 d (data not shown).

After the sciatic nerve was crushed, the amount of N-CAM increased in the soleus muscle (a predominantly slow twitch muscle; 22, 35) from 3 to 11 d; it returned to control levels by 19 d (Fig. 8 *A*, lanes *1–4*). A transient increase of N-CAM was observed at 3 d in the gastrocnemius, but the level was substantially decreased by 7 d (Fig. 8 *A*, lanes *5–8*). The same pattern was observed in another fast twitch muscle, the extensor digitorum longus (Fig. 8 *A*, lanes *9–12*; 16), sug-

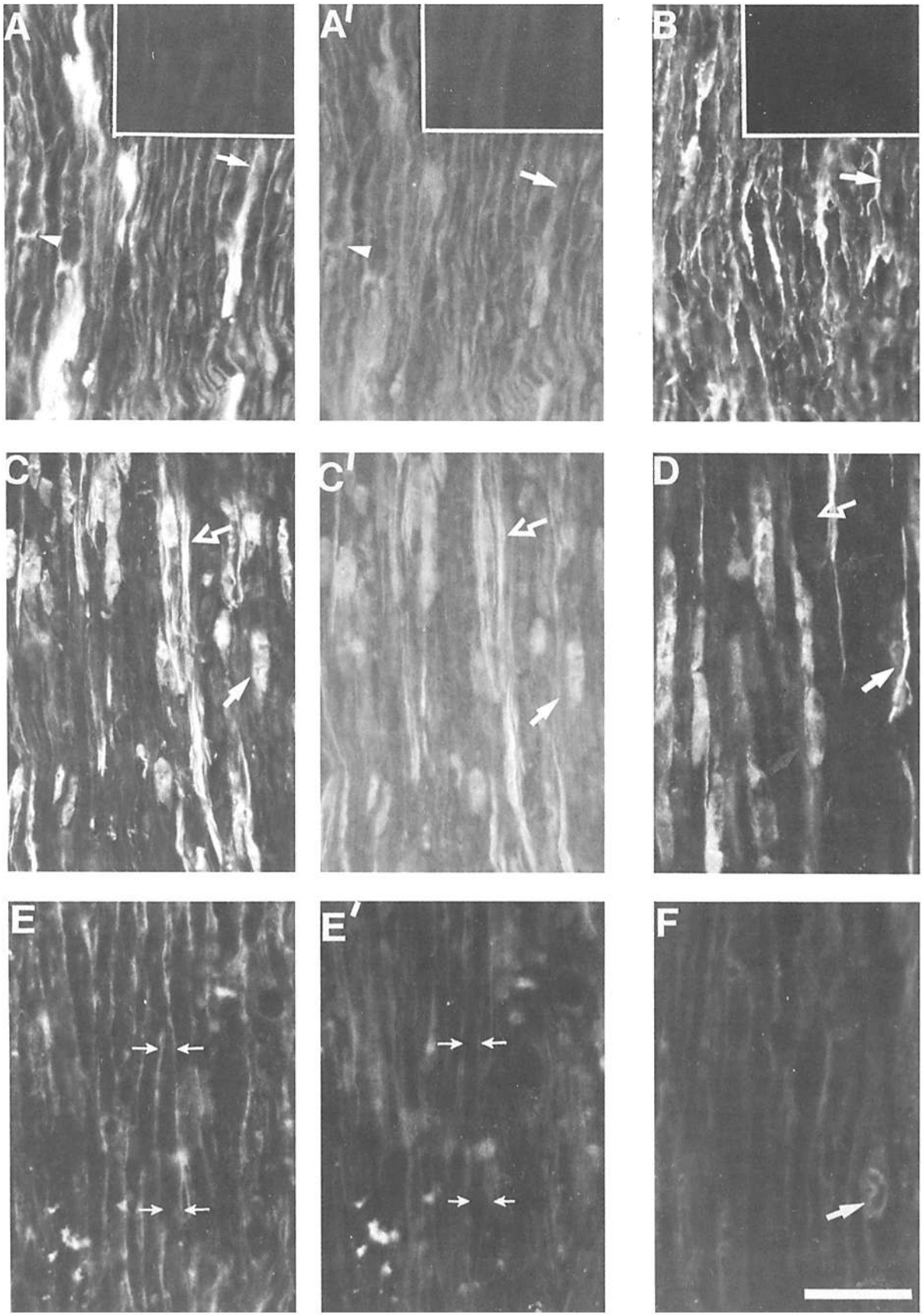
A
A'
B
C
C'
D
E
E'
F

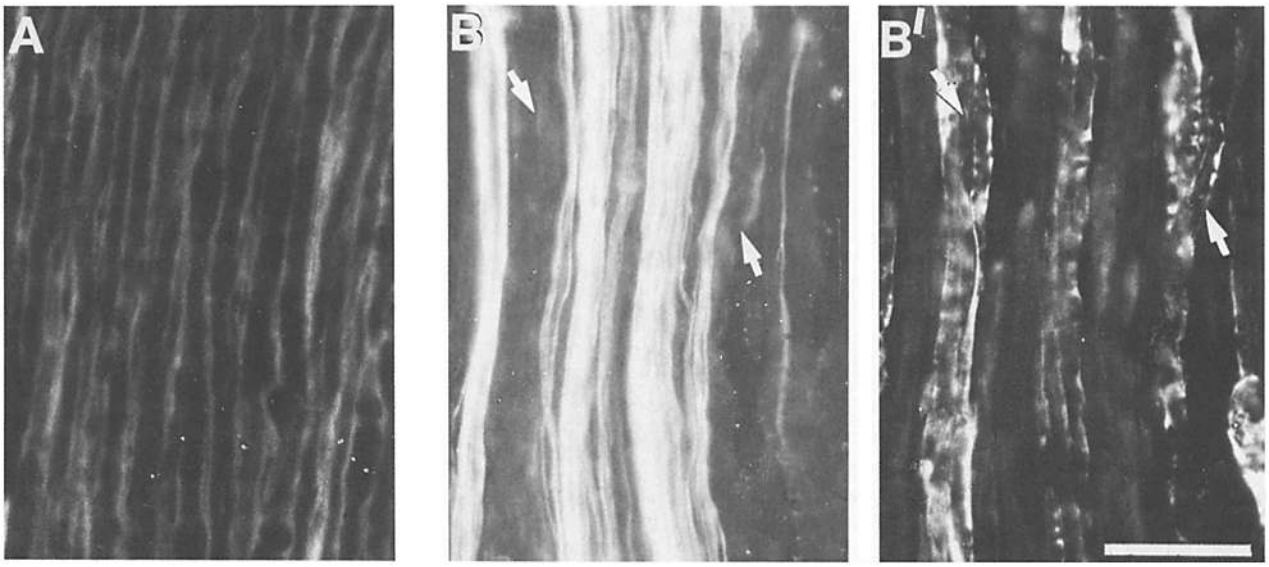

Figure 4. Longitudinal sections of the distal stump of transected nerves after 3 and 20 d stained for anti-Ng-CAM (*A* and *B*) and anti-S100 protein (*B'*). (*A*) After 3 d, thin-walled structures that were probably endoneurial tubes were Ng-CAM positive, and no sprouted nerve fibers had entered the distal stump. However, after 20 d many Ng-CAM–positive nerves traversed the distal stump (*B*). In the same section, cords of S100 protein–labeled Schwann cells (*filled arrows* in *B* and *B'*) formed the bands of Bünger. Bar, 50 μm.

gesting that the transient increase in the amount of N-CAM found in fast twitch muscles disappeared more rapidly than that observed in a slow twitch muscle (soleus).

In immunoblots of normal adult chicken gastrocnemius muscles, N-CAM reactivity appeared in a region of M_r 140,000–200,000; (Fig. 8 *B*, lane *1*). After neuraminidase treatment, a single band of M_r 140,000 was observed (Fig. 8 *B*, lane *2*), indicating that the form of N-CAM found in these muscles is extensively polysialylated (E form), as previously shown in the case of N-CAM from embryonic and neonatal brain and muscle (15, 26, 72). During the first 10 d after the nerve was crushed, the amount of the E form of N-CAM increased, but after 20 and 50 d it diminished progressively (Fig. 8 *B*, lanes *3–6*). This increase extended over the same time course as that established for the reinnervation of the chick hindlimb where endplate potentials are observed in essentially all fibers after 30 d (5, 57). After sciatic nerve transection, the amount of N-CAM was dramatically increased by 10 d (Fig. 8 *B*, lane *7*), remained high after 20 d (Fig. 8 *B*, lane *8*), and diminished by 60 d (Fig. 8 *B*, lane *9*). As observed after nerve crush, the amount of E form and of N-CAM was also increased during this time. Levels similar to those of control muscles were observed 150 d after the nerve was cut (Fig. 8 *B*, lane *10*).

After nerve transection, there was more N-CAM per unit of total protein even at the earliest survival times of 10–60 d (Fig. 9). The time course for the recovery of normal levels of N-CAM was rapid for crush lesions, in which relatively normal levels (ratio of experimental to normal = 1.5) were restored after 50 d. In transected nerves, lower levels (ratio of experimental to normal = 1.3) were apparent only after 150 d (Fig. 9).

To test definitively whether the restoration of normal levels of N-CAM after injury is dependent on reinnervation, we compared the level of N-CAM expression in normal muscles, in muscles that were reinnervated after nerve transection or crush, and in muscles that were maintained in a denervated state (6, 22) by reverse suturing of the transected nerve (41, 44, 45). The extent of innervation in each of these cases was assessed by determining the level of ChAT using a radiochemical assay. In developing muscle, levels of ChAT, the rate-limiting enzyme in the production of acetylcholine, have been shown to reflect the extent of innervation (14). Amounts of this enzyme correlate well with electrophysiological activity in denervated muscle, and are a reliable indicator of the degree of reinnervation (Harris, A. J., F. Rieger, M. Pinçon-Raymond, and L. Houenou, manuscript in preparation).

Table I shows that changes in the levels of N-CAM in these preparations for times up to 30 d were inversely related to the degree of reinnervation as assessed by ChAT activity. We found that ChAT activity decreased to ~30% of control lev-

Figure 3. Longitudinal sections of normal (*A–B*), crushed (*C–D*), and cut nerves (*E–F*) stained for Ng-CAM (*A*, *C*, and *E*), N-CAM (*A'*, *C'*, and *F*) and S100 protein (*B*, *D*, and *F*). In double-labeled sections, Schwann cells (*filled arrows*) expressed Ng-CAM (*A*) and N-CAM (*A'*) and were S100 protein–positive (*B*) in a section taken ~20 μm away. Nonmyelinated fibers were intensely labeled for both CAMs and appeared as discontinuous bundles (*A* and *A'*). Nodes of Ranvier (*arrowheads* in *A* and *A'*) also expressed both CAMs. *Insets A* and *A'*, Ng-CAM and N-CAM staining respectively, with antibodies that were preincubated with purified antigen. *Inset B*, background staining obtained when primary antibodies were omitted from the staining protocol. 3 d after crushing the nerve, Schwann cells (*filled arrows*) were labeled for both Ng-CAM (*C*) and N-CAM (*C'*) several millimeters distal to the crush site; they were also positive for S100 protein (*D*). Sprouted fibers (*open arrows*) were positive for Ng-CAM (*C*) and N-CAM (*C'*) and negative for S100 protein. 3 d after nerve transection, longitudinally oriented structures that were probably endoneurial tubes (between *small arrows* in *E*), were Ng-CAM positive. The same structures were either faintly labeled or negative for N-CAM (*E'*). After 3 d, only occasional S100 protein–positive Schwann cells were apparent in the distal stump (*F*). Bar, 50 μm.

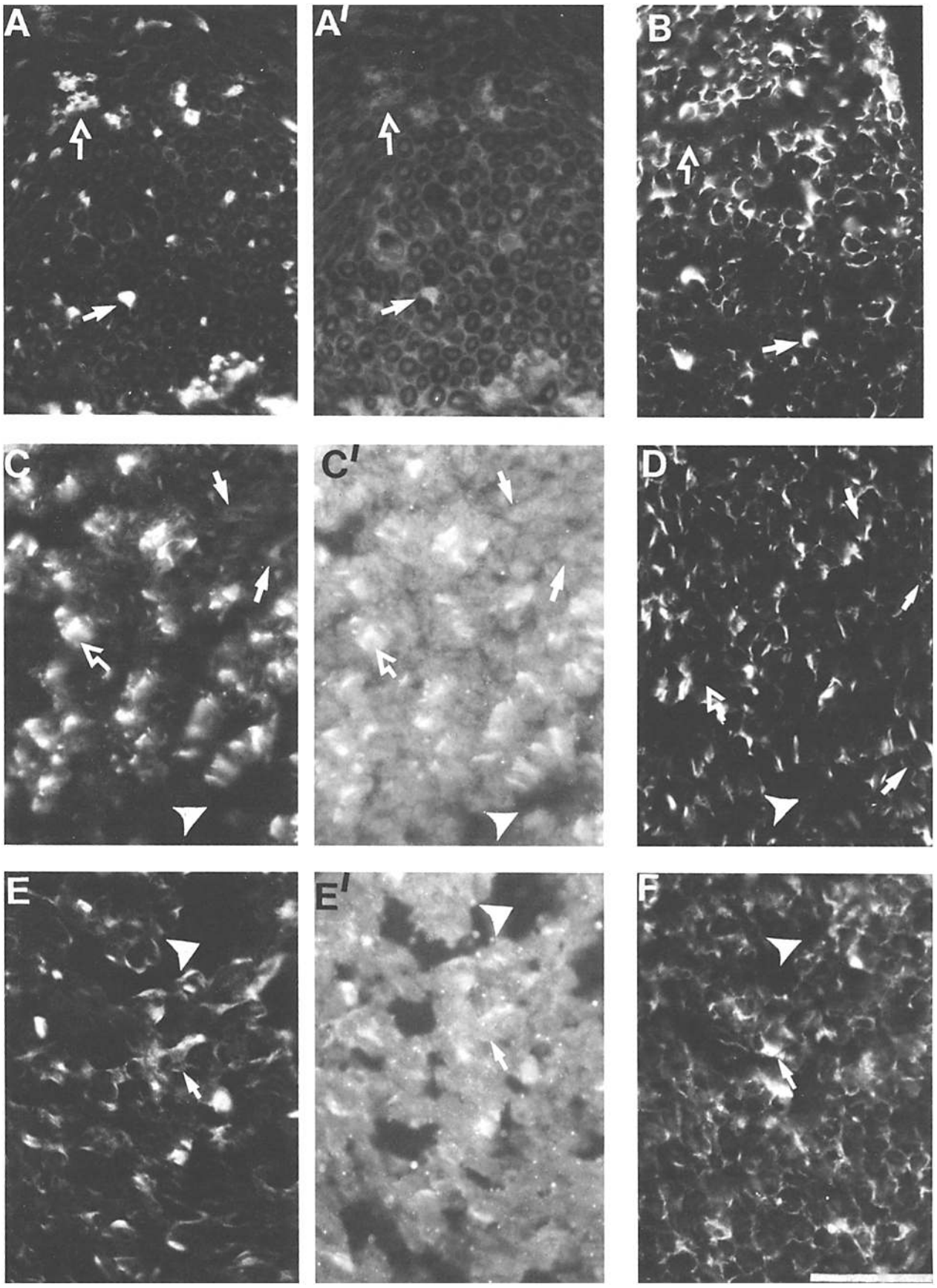
A
A'
B
C
C'
D
E
E'
F

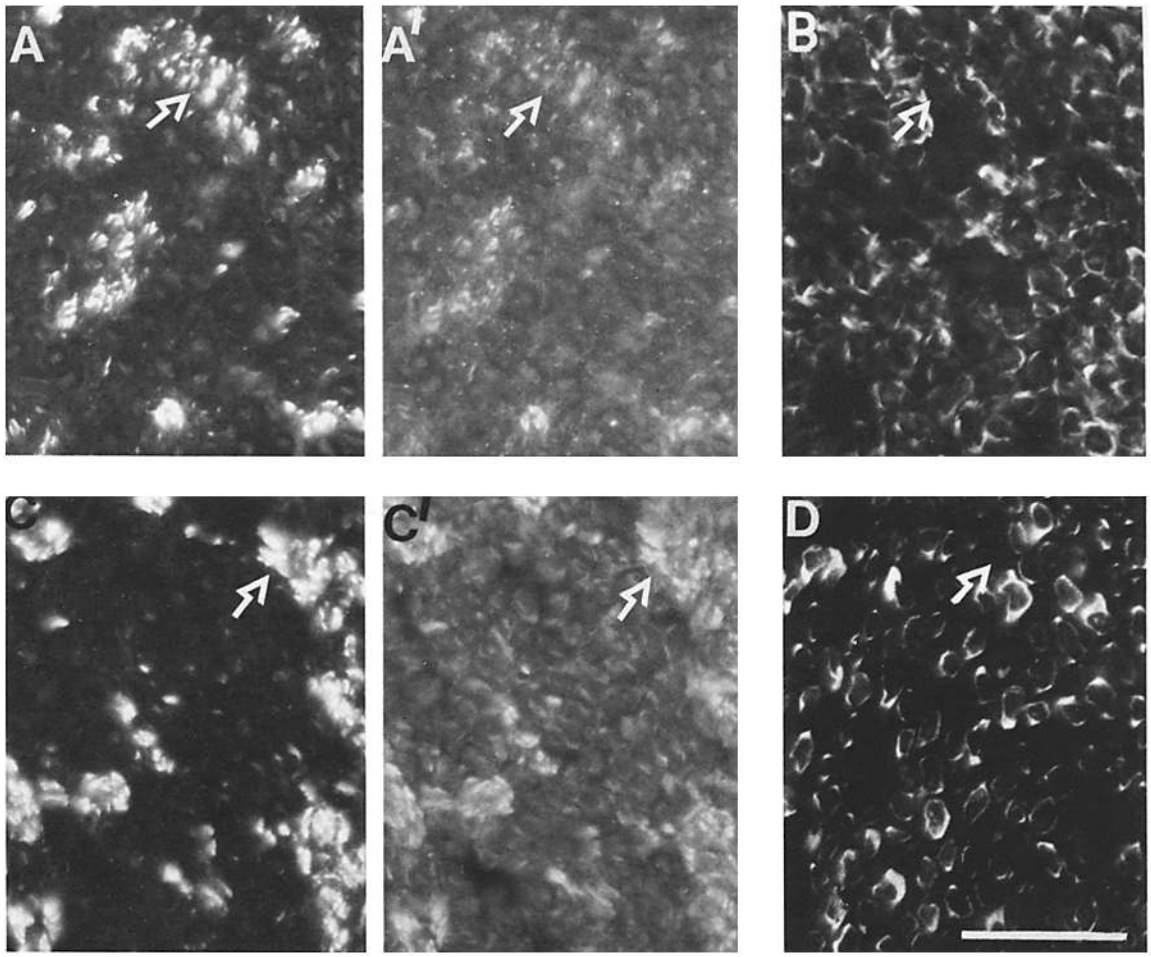

Figure 6. Cross sections of long-term surviving nerves 50 d after crush (*A* and *B*) and 150 d after cut (*C* and *D*). Double-labeled sections indicated that large bundles of nonmyelinated fibers expressed Ng-CAM (*open arrows* in *A* and *C*) and N-CAM (*open arrows* in *A'* and *C'*) after crushing (*A*) or cutting the nerve (*C*). The intensity of Ng-CAM staining approached control levels in the crushed (compare Figs. 6 *A* and 5 *A*) and the cut nerve (compare *A* and *C*), but the intensity of N-CAM was still slightly elevated 50 d after a crush (compare Fig. 6 *A'* to Fig. 5 *A'*) and 150 d after transection (compare Fig. 6 *C'* to Fig. 5 *A'*). The distribution of S100 protein in Schwann cells in times after a crush (*B*, compare to Fig. 5 *B*) more closely resembled the control than the long-term nerves after a transection (*D*). In the latter, more extracellular space seemed to separate individual cells (*D*) than in controls (compare with Fig. 5 *B*). Bar, 50 μm.

els 3 d after transecting, crushing, or reverse-suturing the nerve. After nerve crush, this level increased to 65% by 19 d and remained at this level when assayed at 30 d after injury. Reverse suturing of the nerve successfully prevented reinnervation as indicated by the low levels of ChAT activity that were observed, 10% of normal at both 19 and 30 d after injury. We therefore compared the level of N-CAM expression in muscle when ChAT activity levels had stabilized, at 30 d after injury. After a nerve crush, the extent of reinnervation as indicated by ChAT localization at this time was significant, and the amount of N-CAM was approaching control levels (1.7 times the control). Transected nerves recovered to a lesser extent, as indicated by the lower level of ChAT activity, which was ~40% of control levels, both 19 and 30 d after lesioning the nerves; as expected, N-CAM levels were proportionately higher 30 d after nerve transection (2.5 times the control). More extended analysis over periods up to 6 mo will be required to assess the further changes after

Figure 5. Cross sections of distal segments of normal and injured nerves double-labeled with rabbit anti–Ng-CAM (*A*, *C*, and *E*) and mouse anti–N-CAM IgG (*A'*, *C'*, and *E'*), and an adjacent section stained for S100 protein (*B*, *D*, and *F*). In normal adult nerves, bundles of nonmyelinated axons (*open arrow*) and Schwann cells (*filled arrow*) were intensely stained for Ng-CAM (*A*) and were also N-CAM positive (*open arrow* in *A'*). The myelinated axons were the central CAM-positive regions within unstained toroid-like structures, which represent the myelin sheath (*A* and *A'*). Only Schwann cells (*filled arrow*), and not fibers (*open arrow*), expressed S100 protein (*B*). In the distal stump 10 d after nerve crush (*C* and *D*), axons (*open arrow*) and S100 protein-positive Schwann cells (*filled arrows* in *D*) continue to express Ng-CAM (*C*) and N-CAM (*C'*). The intensity of N-CAM staining was higher than normal (compare *C'* and *A'*), and occasional gaps (*filled arrowheads* in *C*, *C'*, and *D*) appeared within the nerve. 10 d after the nerve was cut, many abnormal spaces (*arrowheads* in *E*, *E'*, and *F*) were seen in the nerve. Ng-CAM staining was most intense in Schwann cells (*filled arrow* in *E*). The overall intensity of N-CAM staining (*E'*) was greater than in controls (*A'*). Although all components of the nerve appeared to express N-CAM at this time (*E'*), the S100 protein staining pattern indicated that the most intense staining was associated with Schwann cells (*arrow* in *F*). Bar, 50 μm.

Table I. Relationship Between N-CAM Expression and Innervation in Mouse Gastrocnemius Muscles as Measured by ChAT activity

Preparation*	Assay procedure	
	ChAT activity‡	Amount of N-CAM§
Normal	1005 ± 81	100 ± 11
30-D crush	639 ± 135	177 ± 11
30-D cut	353 ± 97	249 ± 47
30-D reverse suture	80 ± 84	427 ± 7

Extracts were prepared from normal muscles, or muscles from lesioned animals 30 d after injury. The significance of the correlation between the amount of N-CAM and ChAT activity in individual extracts was evaluated by calculating the Pearson product moment correlation coefficient. The coefficient of −0.948 that was obtained indicated that these two sets of data were strongly and inversely correlated.

* Aliquots taken from the same muscle extracts were assayed for both ChAT activity and amount of N-CAM.

‡ The extent of innervation was assessed by measuring ChAT activity using a radiochemical assay (30); numbers reflect specific counts per minute.

§ The amount of N-CAM in the extracts was determined by quantitative immunoblotting as described in Materials and Methods, and numbers reflect counts per minute. Each number reflects an average value of three different experimental animals ± SD.

transection injuries. In muscles that were chronically denervated by reverse suturing the nerve, the amount of N-CAM was significantly higher than that of cut nerves as well as of control nerves (4.3 times the control). These results are consistent with the interpretation that the level of N-CAM expression in muscle is determined by the degree of innervation.

Nerve. In the normal peripheral nerve of chickens, N-CAM appeared mainly as a major component of M_r 140,000 and a faint polydisperse region extending from M_r 120,000–200,000 representing E form (Fig. 10 *A*, lane *1*). Ng-CAM appeared mainly as a single component of M_r 135,000 (Fig. 10 *B*, lane *1*). When crushed nerves were analyzed biochemically, the amount of N-CAM was higher than normal both after 10 and 20 d of survival; the intensity of both the high molecular weight E form and the M_r 140,000 component increased (Fig. 10 *A*, lanes *2* and *3*). At 50 d, the amount of N-CAM had begun to decrease, although it was slightly elevated above control values (Fig. 10 *A*, lane *4*). The amount of Ng-CAM was also elevated at 10 and 20 d (Fig. 10 *B*, lanes *2* and *3*), but after 50 d, the level of Ng-CAM approached that observed in control nerves (Fig. 10 *B*, compare lane *4* with lane *1*).

At the site of the cut 10 d after nerve transection, N-CAM accumulated primarily in the E form (Fig. 10 *A*, lane *5*), representing a change from the normal pattern. At this time, Schwann cells are the major cellular elements present in this region inasmuch as sprouting fibers have not yet reentered the distal region. This suggests that Schwann cells may be producing the E form of N-CAM. By 60 d, the levels of N-CAM had decreased but the E form persisted (Fig. 10 *A*, lane *6*). The amount of N-CAM approximated control levels after 150 d (Fig. 10 *A*, lane *7*). In long-term survivors (60 and 150 d), the material analyzed included that from regenerated axons in addition to the Schwann cells and connective tissues that predominated in tissues at the shorter survival times.

Ng-CAM also accumulated at the site of the cut, and appeared in increased amounts as a main component of M_r 135,000 both 10 and 60 d after the transection (Fig. 10 *B*, lanes *5* and *6*). After a 150-d recovery period, the level of Ng-CAM resembled that expressed by control nerves (com-

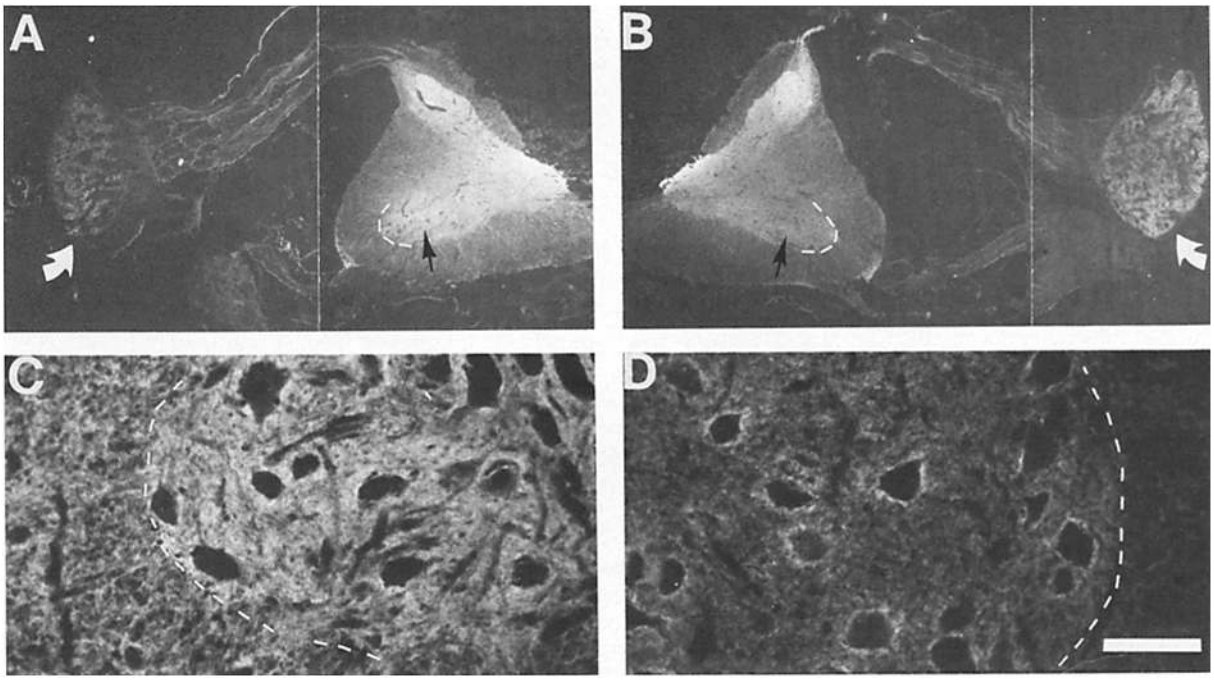

Figure 7. Cross sections of the lowest lumbar segment of spinal cord and DRG 20 d after cutting the sciatic nerve. Control side (*A* and *C*) and experimental side (*B* and *D*) were stained with anti-Ng-CAM (*A* and *B*) and anti-N-CAM antibodies (*C* and *D*). The ventral horn is outlined by a dashed white line. On the experimental side, the intensity of Ng-CAM staining decreased in the ventral horn (*black arrow* in *B*) and increased within the ganglia (*white curved arrow* in *B*). At higher magnification, anti-N-CAM antibodies stained the neuropil of the control (*C*) more intensely than the experimental ventral horn (*D*) where intense N-CAM staining was observed surrounding the motor neurons (*D*). Bar, 80 μm *C* and *D*, and 800 μm for *A* and *B*.

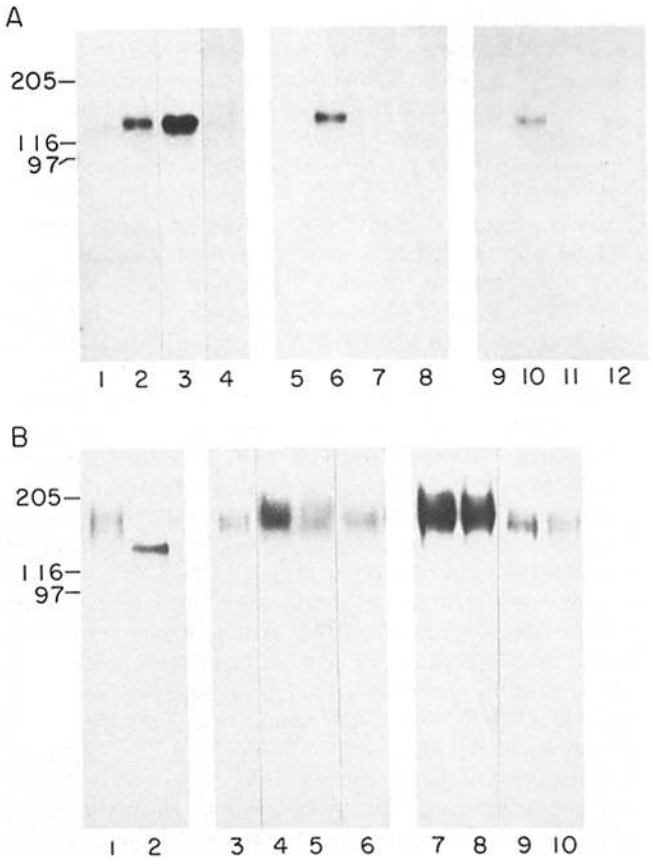

Figure 8. N-CAM in muscle extracts from mice (*A*) and chickens (*B*) after transecting or crushing sciatic nerve. Muscles were dissected at various survival times, extracted, resolved on SDS PAGE (100 μg protein), and then immunoblotted with polyclonal anti-N-CAM IgG (20 μg/ml) as described in Materials and Methods. (*A*) Soleus (lanes *1–4*), gastrocnemius (lanes *5–8*), and extensor digitorum longus muscles (lanes *9–12*). Extracts from control mice (lanes *1*, *5*, and *9*) contained low levels of N-CAM that migrated as a discrete protein of M_r 140,000; this form was only detected in very long autoradiographic exposures. These controls were compared with samples taken 3 d (lanes *2*, *6*, and *10*), 7 d (lanes *3*, *7*, and *11*), and 19 d (lanes *4*, *8*, and *12*) after crushing the sciatic nerve. Levels of N-CAM were increased at both 7 and 19 d in the soleus, a predominantly slow twitch muscle; a response that was of shorter duration was found in gastrocnemius and extensor digitorum longus which are fast muscles. (*B*) N-CAM precipitated from normal chicken gastrocnemius muscle without (lane *1*) or with neuraminidase treatment (lane 2), indicating that the normal form of N-CAM in chicken is sialylated. Extracts from control adult chicken gastrocnemius (lane *3*) were compared with extracts taken from muscles 10 d (lane *4*), 20 d (lane *5*), and 50 d (lane *6*) after the nerve was crushed and 10 d (lane *7*), 20 d (lane *8*), 60 d (lane *9*), and 150 d (lane *10*) after the nerve was cut. Migration of standard proteins is indicated by $M_r \times 10^{-3}$.

pare Fig. 10 *B*, lane *7* with lane *1*). Axonal transport and axoplasmic streaming continue after nerve transection and result in an outflow of cytoplasmic material into the extracellular space (43, 60); either axoplasmic outflow or the synthesis of CAMs by Schwann cells could account for the higher amounts of CAMs in the scar region.

Spinal Cord and DRGs

In the samples analyzed biochemically, neither the amounts

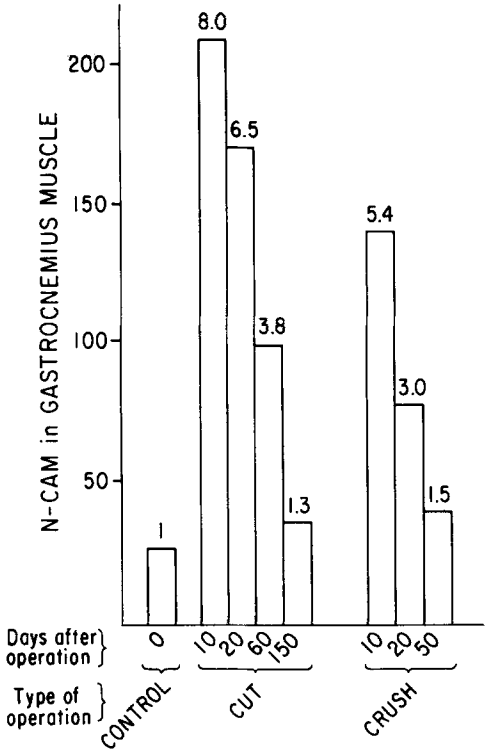

Figure 9. Quantitation of polyclonal anti-N-CAM immunoreactivity in muscle extracts at different times after denervation. The numbers above each bar represent the relative weights of peaks obtained by scanning the autoradiographs in Fig. 8 *B*.

nor the forms of either CAM were detectably altered by crushing or cutting the sciatic nerve (not shown). The changes in the distribution of CAMs found by immunofluorescent staining in fixed sections of spinal cord and DRGs most likely reflect changes that were too local and microscopic to be detected biochemically.

Discussion

In the present investigation, we have found marked local changes in the expression of two well characterized neuronal CAMs after peripheral nerve injury. Comparisons of the observed changes in CAM expression during regeneration with their expression on developing and adult tissues (15, 21, 26, 70, 76, 77) confirmed that CAM expression is radically altered within interacting tissues during regeneration. To identify signals related to nerve repair that could affect CAM expression, it is particularly important to correlate the present observations with other key events in the temporal course of degeneration and regeneration that have been previously described by other workers. The time course of a number of the degenerative and regenerative responses to peripheral nerve section, based on studies of sciatic nerve transection, is compared with that of CAM changes in Fig. 11.

Previous studies (17, 18, 70) suggested that N-CAM expression is regulated by functional contact with the nerve. This conclusion is strongly supported by the present studies in which the time course of CAM expression was closely correlated with the extent of innervation, as measured by ChAT activity. In addition, we found that N-CAM levels remained high in muscles that were chronically denervated, indicating

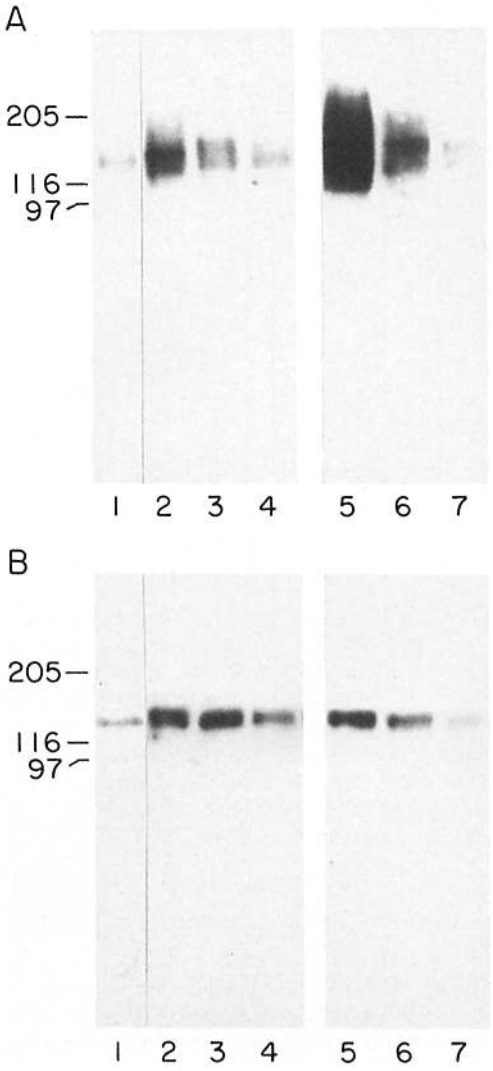

Figure 10. N-CAM and Ng-CAM in chicken sciatic nerve at different survival times after a crush or a cut. Approximately 2-mm portions of the nerve, which included the site of the crush or the scar, were removed. Extracts were resolved on SDS PAGE (100 μg total protein) and immunoblotted with polyclonal antibodies against N-CAM (*A*) and Ng-CAM (*B*). Normal nerve extracts (lane *1*) were compared with extracts taken from nerves 10 d (lane *2*), 20 d (lane *3*), and 50 d (lane *4*) after crushing the nerve and 10 d (lane *5*), 60 d (lane *6*), and 150 d (lane *7*) after nerve transection. Migration of standard proteins is indicated by $M_r \times 10^{-3}$.

that restoration to normal levels of N-CAM requires reinnervation. However, the present data also suggested that the expression of muscle N-CAM in response to nerve transection may be more complex in some sites than was previously assumed (70). For example, in chickens, control levels were restored 150 d after the nerve was cut, despite the fact that many muscle fibers are never reinnervated (6, 16, 67, 74).

It was striking that elevated levels of both N-CAM and Ng-CAM were observed in Schwann cells after the sciatic nerve was injured. During this period, the Schwann cells proliferate and migrate (1, 47, 84; and Fig. 11), and it is possible that the increased production of Ng-CAM in these cells enhances the migratory activity toward the injury site, comparable to the expression of Ng-CAM by migrating neurons (21, 38). Binding of CAMs on adjacent Schwann cells may be involved in the formation of bands of Büngner. It is also possible that the Ng-CAM found within endoneurial tubes provides a favorable substrate for the extension of regenerating axons. The amounts of both N-CAM and Ng-CAM return to near normal levels in nerves at about the same time (60 d) that myelination begins (2, 45, 66; and Fig. 11). Thus, the reestablishment of relatively low levels of CAM synthesis may be an early event preceding myelination.

In the regenerating sciatic nerve, the form of N-CAM expressed was similar to the sialic acid-rich, diffusely migrating E form of N-CAM found in embryonic brain (15, 26). The form of N-CAM seen in regeneration appeared to have less sialic acid than the E form, but significantly more than the M_r 140,000 form present in the mature tissue before injury. The increase in the polydisperse form may have originated locally from Schwann cells that are induced to proliferate extensively after nerve injury (1, 66). Alternatively, the injury may have triggered changes in the synthesis of N-CAM by the motor neurons of the spinal cord and the CAMs may have accumulated in the scar region from the cut end of the nerves. The A forms of N-CAM that appear later probably originate from the ingrowing axons themselves, because the staining results indicated that unmyelinated fiber bundles expressed much more N-CAM than any other components in the region analyzed.

Correlation of the changes in CAM expression in the spinal cord with events known to be occurring during regeneration suggests possible origins for these changes (Fig. 11). Both neuronal CAMs were localized at the cell surface of spinal cord motor neurons coincident with established times of motor neuron sprouting (11). A similar pattern of Nissl stained granules has been observed at the periphery of denervated motor neurons, but only after peripheral nerve transection, suggesting that the phenomenon may be related to neuron degeneration (13). However, this pattern was maintained long after chromatolysis was complete, and may therefore also be associated with neuron recovery and the increased production of protein components of the cell membrane (54).

The finding that the changes in CAM expression induced by transection or by a crush differed mainly in their time course suggested that similar signals regulate CAM expression regardless of the nature of the nerve injury. Nonetheless, several differences were found in the consequences of each kind of lesion, including the distinctive pattern of N-CAM and Ng-CAM reactivity observed in the spinal cord, DRG, and scar region only in transected nerves and not after a nerve crush. Levels of both N-CAM and Ng-CAM return to normal faster after crush than transection. These findings are in accord with those found previously: recovery is far more rapid and complete after nerve crush than nerve cut (66, 67, 69). Most animal species respond with very similar rates of regeneration after a nerve crush (60) and almost all muscle fibers are reinnervated (67). After a nerve cut, however, large numbers of spinal cord and DRG neurons die, and fewer muscle fibers become reinnervated (67).

Several observations in these studies suggested that changes induced in CAM expression during regenerative responses were not simply a recapitulation of normal developmental processes. We did observe a change in the form of N-CAM during the regeneration of sciatic nerves that mimicked early development, suggesting that the E form has a significant

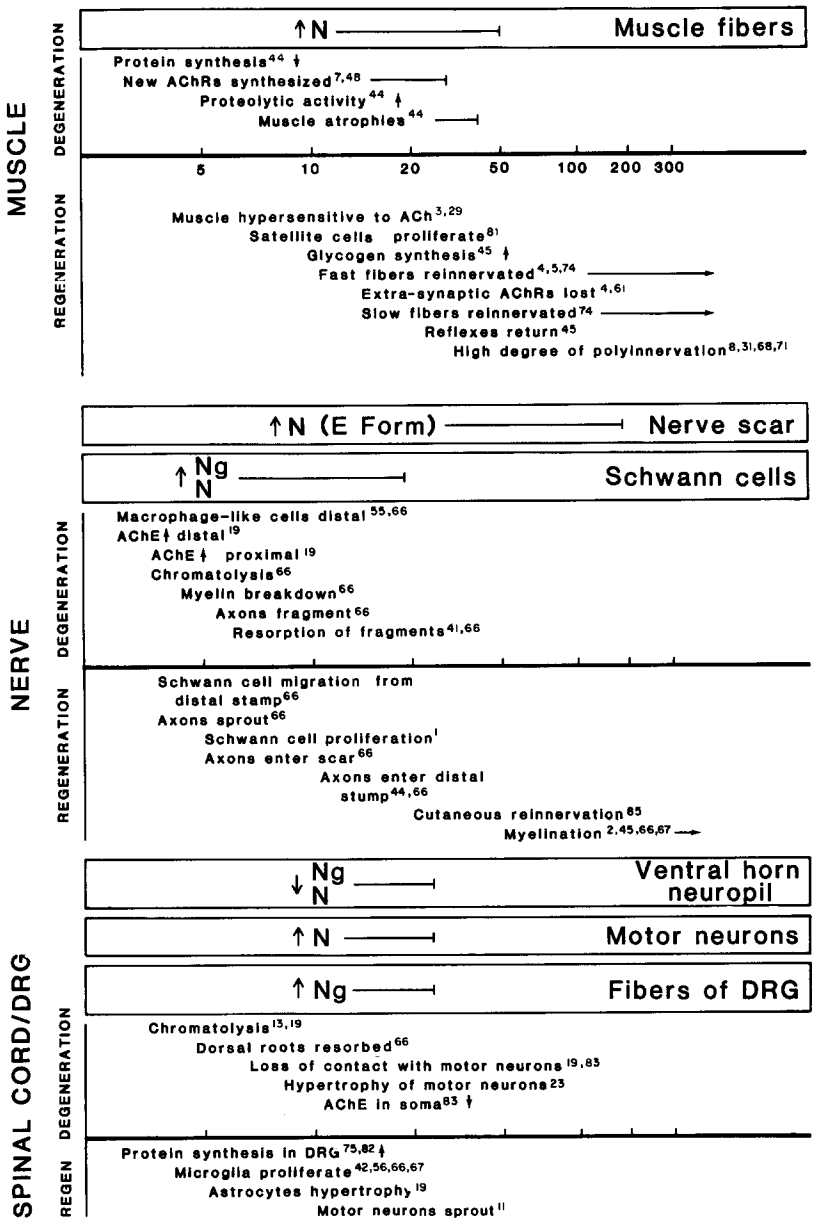

Figure 11. Summary diagram correlating the time course of established degenerative and regenerative phenomena after peripheral nerve transection with changes in CAM expression. Summaries of the changes in CAM expression are enclosed within the bars and labeled for each tissue, irrespective of species, although particular attention was paid to the responses in birds. Responses of skeletal muscles (*top*), peripheral nerves (*middle*), and spinal cord/dorsal root ganglia (*bottom*) are shown. The abscissa represents time in days; degenerative phenomena are summarized above it and regenerative phenomena are placed below it. The duration of each response is represented by the approximate length of each written phrase, or by the length of horizontal lines; the initiation of each process is approximated by the starting point of each phrase. The termination point corresponds to a return to nearly normal levels. Increases in CAM expression are indicated by upward arrows and decreases by downward arrows. Superscripts are reference numbers. Responses that continue beyond 300 d are indicated by arrows.

role in nerve repair. However, if regenerative processes represented simple recapitulation of development, this transition would have been expected in all regions. It only occurred, however, in the neighborhood of the injured area of the nerve, underlining the difference between developmental and regenerative processes.

The present observations provide additional strong support for the notion that CAM expression is coupled to morphology and they show that alterations in morphology result in dramatic changes in CAM expression characteristic of particular regions in a linked neuromuscular system. Conversely, it has been found that morphology depends upon CAM-mediated cell–cell interactions. For example, the application of antibodies against N-CAM at appropriate times of development disrupts formation of retinal laminae (12), neuron–myotube contacts (72) and the mapped connection between the retina and tectum (32). In the last case, the retino-tectal map is gradually restored in time, suggesting the occurrence of dynamic regulation of structure as anti-N-CAM Fab' is depleted.

All of these studies suggest the existence of a complex signaling system relating morphology to CAM expression and to cell differentiation in both development and differentiation. Although the nature of the signals remains unknown, recent observations indicate that Ng-CAM expression, but not N-CAM expression, increases in PC12 cells exposed to NGF (34), suggesting that neurotrophic factors can provide such signals. CAM expression in development thus may be linked to several important steps in cell differentiation that are dependent on neurotrophic factors; similar hormonal or trophic influences may act during regeneration. Although the mode of action of such signals is not known, preliminary experiments, based on the finding that N-CAM expression and function are decreased in retinal cell lines infected with Rous sarcoma virus, indicate that primary control of N-CAM occurs at the transcriptional level (36). In addition, posttransla-

tional controls may also be involved in the modulation of CAMs; for example, E to A conversion results from synthesis of new molecules containing lower amounts of polysialic acid (33). Furthering our understanding of such mechanisms and of signals that operate to govern cell adhesion during development and repair of the peripheral nervous system is likely to have practical applications, particularly in attempts to alleviate injury or alter regeneration.

We are deeply grateful for the extensive analysis and criticism of the data and the written text by Drs. Kathryn L. Crossin and Robert B. Brackenbury. We thank Dr. Martine Pinçon-Raymond for help in the mouse denervation experiments.

This research was supported by a Senator Jacob Javits Center of Excellence in Neuroscience Grant (No. NS-22789), by National Institutes of Health grants HD-09635, AM-04256, and NS-21629, and by funds from Institut National de la Santé et de la Recherche Médicale, and Fondation pour la Recherche Médicale. Postdoctoral Fellowships NS07636-01 and EMBO No. ALTF 11-1984 were awarded to Joanne K. Daniloff and Giovanni Levi.

Received for publication 23 December 1985, and in revised form 1 May 1986.

References

1. Abercrombie, M., and M. L. Johnson. 1946. Quantitative histology of Wallerian degeneration. *J. Anat.* 80:37–47.

2. Alberghina, M., M. Viola, and A. M. Giuffrida. 1984. Myelination process in the rat sciatic nerve during regeneration and development. *Neurochem. Res.* 9:887–902.

3. Axelsson, J., and S. Thesleff. 1959. A study of supersensitivity in denervated mammalian skeletal muscle. *J. Physiol. (Lond.).* 147:178–193.

4. Bennett, M. R., M. McLachlan, and R. S. Taylor. 1973. Formation of synapses in reinnervated mammalian striated muscle. *J. Physiol. (Lond.).* 233: 481–500.

5. Bennett, M. R., A. G. Pettigrew, and R. S. Taylor. 1973. The formation of synapses in reinnervated and cross-reinnervated adult avian muscle. *J. Physiol. (Lond.).* 230:331–357.

6. Benoit, P., and J. P. Changeux. 1978. Consequences of blocking the nerve with a local anesthetic on the evolution of multiinnervation at the regenerating neuromuscular junction of the rat. *Brain Res.* 149:89–96.

7. Berg, D. K., R. B. Kelly, P. B. Sargent, P. Williamson, and Z. W. Hall. 1972. Binding of a α-bungarotoxin to acetylcholine receptors in mammalian muscle. *Proc. Natl. Acad. Sci. USA.* 69:147–151.

8. Bernstein, J. J., and L. Guth. 1961. Nonselectivity in the establishment of neuromuscular connections following nerve regeneration in the rat. *Exp. Neurol.* 4:262–275.

9. Bock, E., C. Richter-Landsberg, A. Faissner, and M. Schachner. 1985. Demonstration of immunochemical identity between the nerve growth-inducible large external (NILE) glycoprotein and the cell adhesion molecule L1. *EMBO (Eur. Mol. Biol. Organ.) J.* 4:2765–2768.

10. Brackenbury, R., U. Rutishauser, and G. M. Edelman. 1981. Distinct calcium-independent and calcium-dependent adhesion systems of chicken embryo cells. *Proc. Natl. Acad. Sci. USA.* 78:387–391.

11. Brushart, T. M., and M. M. Mesulam. 1980. Alterations in connections between muscle and anterior horn motor neurons after peripheral repair. *Science (Wash. DC).* 208:603–605.

12. Buskirk, D. R., J.-P. Thiery, U. Rutishauser, and G. M. Edelman. 1980. Antibodies to neural cell adhesion molecules disrupt histogenesis in cultured chick retina. *Nature (Lond.).* 285:488–489.

13. Cavanaugh, M. W. 1951. Quantitative effects of the peripheral innervation area on nerves and spinal ganglion cells. *J. Comp. Neurol.* 94:181–219.

14. Chiappinelli, V., E. Giacobini, G. Pilar, and H. Uchimura. 1976. Induction of cholinergic enzymes in chick ciliary ganglion and iris muscle cells during synapse formation. *J. Physiol. (Lond.).* 257:749–766.

15. Chuong, C.-M., and G. M. Edelman. 1985. Alterations in neural cell adhesion molecules during development of different regions of the nervous system. *J. Neurosci.* 4:2364–2368.

16. Close, R. 1965. Effects of cross-union of motor nerves to fast and slow skeletal muscles. *Nature (Lond.).* 206:831–832.

17. Covault, J., and J. Sanes. 1985. Neural cell adhesion molecule (N-CAM) accumulates in denervated and paralyzed skeletal muscles. *Proc. Natl. Acad. Sci. USA.* 82:4544–4548.

18. Covault, J., and J. Sanes. 1986. Distribution of N-CAM in synaptic and extrasynaptic portions of developing and adult skeletal muscle. *J. Cell Biol.* 102:716–730.

19. Cragg, B. G. 1970. What is the signal for chromatolysis? *Brain Res.* 23:1–21.

20. Cunningham, B. A., S. Hoffman, U. Rutishauser, J. J. Hemperly, and G. M. Edelman. 1983. Molecular topography of the neural cell adhesion molecule N-CAM: surface orientation and location of sialic acid-rich and binding regions. *Proc. Natl. Acad. Sci. USA.* 80:3116–3120.

21. Daniloff, J. K., C.-M. Chuong, G. Levi, and G. M. Edelman. 1986. Differential distribution of cell adhesion molecules during histogenesis of the chick nervous system. *J. Neurosci.* 6:739–758.

22. Duchen, L. W. 1979. Hereditary disorders of motor and sensory neurons in the mouse. *Ann. NY Acad. Sci.* 317:506–511.

23. Ducker, T. B. 1972. Metabolic factors in surgery of peripheral nerves. *Surg. Clin. North Am.* 52:1109–1122.

24. Edelman, G. M. 1983. Cell adhesion molecules. *Science (Wash. DC).* 219:450–457.

25. Edelman, G. M. 1984. Modulation of cell adhesion during induction, histogenesis, and perinatal development of the nervous system. *Annu. Rev. Neurosci.* 7:339–377.

26. Edelman, G. M., and C.-M. Chuong. 1982. Embryonic to adult conversion of neural cell adhesion molecules in normal and *staggerer* mice. *Proc. Natl. Acad. Sci. USA.* 79:7036–7040.

27. Emmelin, N., I. Nodenfelt, and C. Perec. 1966. Rate of fall of choline acetyltransferase activity in denervated diaphragms is dependent on the length of the degenerating nerve. *Experientia (Basel).* 22:725–726.

28. Faissner, A., J. Kruse, J. Nieke, and M. Schachner. 1984. Expression of neural cell adhesion molecule L1 during development, in neurological mutants, and in the peripheral nervous system. *Dev. Brain Res.* 15:69–82.

29. Filogamo, G., and G. Gabella. 1966. Cholinesterase behavior in the denervated and reinnervated muscles. *Acta Anat.* 63:199–214.

30. Fonnum, F. 1975. A rapid radiochemical method for the delineation of choline acetyltransferase. *J. Neurochem.* 24:407–409.

31. Frank, E., J. K. S. Jansen, T. Lomo, and R. H. Westgaard. 1975. The interaction between foreign and original motor nerves innervating the soleus muscle of rats. *J. Physiol. (Lond.).* 247:725–743.

32. Fraser, S. E., B. A. Murray, C.-M. Chuong, and G. M. Edelman. 1984. Alteration of the retinotectal map in *Xenopus* by antibodies to neural cell adhesion molecules. *Proc. Natl. Acad. Sci. USA.* 81:4222–4226.

33. Friedlander, D. R., Brackenbury, R., and Edelman, G. M. 1984. Conversion of embryonic form to adult forms of N-CAM in vitro: results from *de novo* synthesis of adult forms. *J. Cell Biol.* 101:412–419.

34. Friedlander, D. R., Grumet, M., and Edelman, G. M. 1986. Nerve growth factor enhances expression of neuron–glia cell adhesion molecule in PC12 cells. *J. Cell Biol.* 102:413–419.

35. Gauthier, G. F., and S. Lowey. 1979. Distribution of myosin isoenzymes among skeletal muscle fibers. *J. Cell Biol.* 81:10–25.

36. Greenberg, M. E., R. Brackenbury, and G. M. Edelman. 1984. Alteration of neural cell adhesion molecule (N-CAM) expression after neuronal cell transformation by Rous sarcoma virus. *Proc. Natl. Acad. Sci. USA.* 81:969–973.

37. Grumet, M., and G. M. Edelman. 1984. Heterotypic binding between neuronal membrane vesicles and glial cells is mediated by a specific cell adhesion molecule. *J. Cell Biol.* 98:1746–1756.

38. Grumet, M., S. Hoffman, C.-M. Chuong, and G. M. Edelman. 1984. Polypeptide components and binding functions of neuron-glia cell adhesion molecules. *Proc. Natl. Acad. Sci. USA.* 81:7989–7993.

39. Grumet, M., S. Hoffman, and G. M. Edelman. 1984. Two antigenically related cell adhesion molecules of different specificities mediate neuron-neuron and neuron-glia adhesion. *Proc. Natl. Acad. Sci. USA.* 80:267–271.

40. Grumet, M., U. Rutishauser, and G. M. Edelman. 1982. N-CAM mediates adhesion between embryonic nerve and muscle cells *in vitro*. *Nature (Lond.).* 295:693–695.

41. Guth, L. 1956. Regeneration in the mammalian peripheral nervous system. *Physiol. Rev.* 36:441–478.

42. Guth, L. 1968. 'Trophic' influences of nerve on muscle. *Physiol. Rev.* 48:645–687.

43. Guth, L., and P. R. Watson. 1967. The influence of reinnervation on the soluble proteins of slow and fast muscles of the rat. *Exp. Neurol.* 17:107–117.

44. Gutman, E. 1964. Neurotrophic relations in the regeneration process. *Prog. Brain Res.* 13:72–112.

45. Gutman, E., and J. Z. Young. 1944. The reinnervation of muscle after various periods of atrophy. *J. Anat.* 78:15–43.

46. Haglid, K. G., A. Hamberger, H.-A. Hansson, H. Hyden, L. Persson, and L. Ronnback. 1976. Cellular and subcellular distribution of the S-100 protein in rabbit and rat central nervous system. *J. Neurosci. Res.* 2:175–191.

47. Hamburger, V. 1948. The mitotic patterns of the spinal cord of the chick embryo and their relation to histogenic processes. *J. Comp. Neurol.* 88: 221–284.

48. Hartzell, H. C., and D. M. Fambrough. 1972. Acetylcholine receptors. Distribution and extra-junctional sensitivity in rat diaphragm after denervation correlated with acetylcholine sensitivity. *J. Gen. Physiol.* 60:284–292.

49. Hoffman, S., and G. M. Edelman. 1983. Kinetics of homophilic binding by embryonic and adult forms of the neural cell adhesion molecule. *Proc. Natl. Acad. Sci. USA.* 80:5762–5766.

50. Hoffman, S., D. R. Friedlander, C.-M Chuong, M. Grumet, and G. M. Edelman. 1986. Differential contributions of Ng-CAM and N-CAM to cell adhesion in different neural regions. *J. Cell Biol.* 103:145–158.

51. Hoffman, S., B. C. Sorkin, B. C. White, R. Brackenbury, R. Mailhammer, U. Rutishauser, B. A. Cunningham, and G. M. Edelman. 1982. Chemical

characterization of a neural cell adhesion molecule purified from embryonic brain membranes. *J. Biol. Chem.* 257:7720–7729.

52. Holton, B., and J. A. Weston. 1982. Analysis of glial cell differentiation in peripheral nervous tissue. I. S100 accumulation in quail embryo spinal ganglion cultures. *Dev. Biol.* 89:64–71.

53. Holton, B., and J. A. Weston. 1982. Analysis of glial cell differentiation in peripheral nervous tissue. II. Neurons promote S100 synthesis by purified glial cell precursor cell populations. *Dev. Biol.* 89:72–81.

54. Hyden, H. 1943. Protein metabolism in the nerve cell during growth and function. *Acta Physiol. Scand.* 17(Suppl.):1–36.

55. Ide, C., K. Tohyama, R. Yokota, T. Nitatori, and S. Onodera. 1983. Schwann cell basal lamina and nerve regeneration. *Brain Res.* 288:61–75.

56. Kreutzberg, G. W. 1982. Acute neural reaction in injury. *Brain Res.* 288:61–75.

57. Letinsky, M. S., K. H. Fishbeck, and U. J. McMahan. 1976. Precision of reinnervation of original postsynaptic sites in frog muscle after a nerve crush. *J. Neurocytol.* 5:691–718.

58. Levi-Montalcini, R., and P. U. Angeletti. 1968. Nerve growth factor. *Physiol. Rev.* 48:534–569.

59. Lowry, O. H., N. J. Rosebrough, A. L. Farr, and R. J. Randall. 1951. Protein measurement with the Folin-phenol reagent. *J. Biol. Chem.* 193:265–275.

60. Lubinska, L. 1964. Axoplasmic streaming in regenerating and normal nerve fibers. *Dev. Biol.* 89:1–71.

61. Miledi, R. 1960. The acetylcholine sensitivity of frog muscle fibers after complete or partial denervation. *J. Physiol (Lond.).* 151:1–23.

62. Nieke, J., and M. Schachner. 1985. Expression of the neural cell adhesion molecules L1 and N-CAM and their common carbohydrate epitope L2/HNK-1 during development and after transection of the mouse sciatic nerve. *Differentiation.* 30:141–151.

63. Noble, M., M. Albrechtsen, C. Moller, J. Lyles, E. Bock, C. Goridis, M. Watanabe, and U. Rutishauser. 1985. Glial cells express N-CAM/D2-CAM-like polypeptides *in vitro. Nature (Lond.).* 316:725–728.

64. Pannese, E. 1969. Electron microscopic study of the development of the satellite cell sheath in spinal ganglia. *J. Comp. Neurol.* 135:381–422.

65. Pinçon-Raymond, M., M. A. Ludowski, J. Cartaud, and F. Rieger. 1983. Intense ultraterminal sprouting from motor nerves and non-junctional sarcolemma of the soleus muscle (slow-twitch) in motor endplate disease in the mouse. *Tissue & Cell.* 15:205–216.

66. Ramon y Cajal, S. 1928. Degeneration and regeneration of the nervous system. Vol. 1. R. M. May, translator and editor. Oxford University Press, London. 1–396.

67. Ramon y Cajal, S. 1928. Degeneration and regeneration of the nervous system. Vol. 2. R. M. May, translator and editor. Oxford University Press, London. 397–769.

68. Redfern, P. A. 1970. Neuromuscular transmission in newborn rats. *J. Physiol. (Lond.).* 209:701–709.

69. Redshaw, J. D., and M. A. Bisby. 1985. Comparison of the effects of sciatic nerve crush or resection on the proteins of fast axonal transport in rat dorsal root ganglion cell axons. *Exp. Neurol.* 88:437–446.

70. Rieger, F., M. Grumet, and G. M. Edelman. 1985. N-CAM at the vertebrate neuromuscular junction. *J. Cell Biol.* 101:285–293.

70a. Rieger, F., J. K. Daniloff, M. Pinçon-Raymond, K. L. Crossin, M. Grumet, and G. M. Edelman. 1986. Neuronal cell adhesion molecules and cytotactin are colocalized at the node of Ranvier. *J. Cell Biol.* In press.

71. Rothshenker, S., and U. J. McMahan. 1976. Altered patterns of innervation in frog muscle after denervation. *J. Neurocytol.* 5:719–730.

72. Rutishauser, U., M. Grumet, and G. M. Edelman. 1983. Neural cell adhesion molecule mediates initial interactions between spinal cord neurons and muscle cells in culture. *J. Cell Biol.* 97:145–152.

73. Schmechel, D., P. J. Marangos, A. P. Zis, M. Brightman, and F. K. Goodwin. 1978. Brain enolases as specific markers of neuronal and glial cells. *Science (Wash. DC).* 199:313–315.

74. Schmidt, H., and E. Stefani. 1976. Reinnervation of fast twitch and slow muscle fibers of the frog after crushing the motor nerves. 1976. *J. Physiol.* 258:99–123.

75. Scott, D., E. Gutman, and P. Horsky. 1966. Regeneration in spinal neurons: proteosynthesis following nerve growth factor administration. *Science (Wash. DC).* 152:787–788.

76. Thiery, J.-P., A. Delouvée, M. Grumet, and G. M. Edelman. 1985. Initial appearance and regional distribution of the neuron-glia cell adhesion molecules in the chick embryo. *J. Cell Biol.* 100:442–456.

77. Thiery, J.-P., J.-L. Duband, U. Rutishauser, and G. M. Edelman. 1982. Cell adhesion molecules in early chicken embryogenesis. *Proc. Natl. Acad. Sci. USA.* 79:6737–6741.

78. Thoenen, H., and D. Edgar. 1985. Neurotrophic factors. *Science (Wash. DC).* 229:238–242.

79. Torrey, T. W. 1934. The relation of taste buds to their nerve fibers. *J. Comp. Neurol.* 59:203–220.

80. Towbin, H. T., T. Staehelin, and J. Gordon. 1979. Electrophoretic transfer of proteins from polyacrylamide gels to nitrocellulose sheets: procedure and some applications. *Proc. Natl. Acad. Sci. USA.* 76:4350–4354.

81. Tower, S. 1937. Atrophy and degeneration in skeletal muscle. *Am. J. Anat.* 46:1–43.

82. Watson, W. E. 1966. Quantitative observations upon acetylcholine hydrolase activity of nerve cells after axotomy. *J. Neurochem.* 13:1549–1550.

83. Watson, W. E. 1966. Alteration of the adherence of glia to neurons following nerve injury. *J. Neurochem.* 13:536–537.

84. Weston, J. A. 1963. A radioautographic analysis of the migration and localization of trunk neural crest cells in the chick. *Dev. Biol.* 6:279–310.

85. Zelena, J. 1964. Development, degeneration and regeneration of receptor organs. *Dev. Biol.* 89:175–213.